Science of the Total Environment 616–617 (2018) 824–840

Contents lists available at ScienceDirect

Science of the Total Environment

journal homepage: www.elsevier.com/locate/scitotenv

Carbon exchanges and their responses to temperature and precipitation in forest ecosystems in Yunnan, Southwest China

Xuehai Fei [a,b,c], Qinghai Song [a,b,*], Yiping Zhang [a,b,*], Yuntong Liu [a,b], Liqing Sha [a,b], Guirui Yu [h], Leiming Zhang [h], Changqun Duan [i], Yun Deng [a,d], Chuansheng Wu [a,e], Zhiyun Lu [a,e], Kang Luo [a,c,e], Aiguo Chen [a,f], Kun Xu [a,g], Weiwei Liu [a,g], Hua Huang [a,g], Yanqiang Jin [a,b,c], Ruiwu Zhou [a,b,c], Jing Li [a,b,c], Youxing Lin [a,b,c], Liguo Zhou [a,b,c], Yane Fu [a,c], Xiaolong Bai [a,c], Xianhui Tang [a,b,c], Jinbo Gao [a,b,c], Wenjun Zhou [a,b], John Grace [j]

[a] Key Laboratory of Tropical Forest Ecology, Xishuangbanna Tropical Botanical Garden, Chinese Academy of Sciences, Menglun, Yunnan 666303, China
[b] Global Change Ecology Group, Xishuangbanna Tropical Botanical Garden, Chinese Academy of Sciences, Menglun 666303, China
[c] University of Chinese Academy of Sciences, Beijing 100049, China
[d] Xishuangbanna Station for Tropical Rainforest Ecosystem Studies, Menglun, Xishuangbanna, Yunnan 666303, China
[e] Ailaoshan Station for Subtropical Forest Ecosystem Studies, Jingdong, Yunnan 676209, China
[f] Yuanjiang Savanna Ecosystem Research Station, Xishuangbanna Tropical Botanical Garden, Chinese Academy of Sciences, Yuanjiang, Yunnan 653300, China
[g] Lijiang Forest Ecosystem Research Station, Kunming Institute of Botany, Chinese Academy of Sciences, 132# Lanhei Road, Heilongtan, Kunming 650201, Yunnan, China
[h] Synthesis Research Center of Chinese Ecosystem Research Network, Key Laboratory of Ecosystem Network Observation and Modeling, Institute of Geographic Sciences and Natural Resources Research, Chinese Academy of Sciences, Beijing 100101, China
[i] Institute of Environmental Sciences and Ecological Restoration, School of Ecology and Environmental Sciences, Yunnan University, Kunming 650091, China
[j] School of GeoSciences, The University of Edinburgh, Edinburgh EH9 3FF, UK

HIGHLIGHTS

- All four ecosystems were carbon sinks although contrasting seasonality of NEP.
- Relationship between NEP and GPP should be parabolic rather than linear.
- Path/redundancy analysis were applied to identify patterns of controls on C fluxes.
- Controls differed: T reduced NEP in rainforest, while P increased NEP in savanna.
- Variations in NEP were more sensitive to T than P in Yunnan's forest ecosystems.

GRAPHICAL ABSTRACT

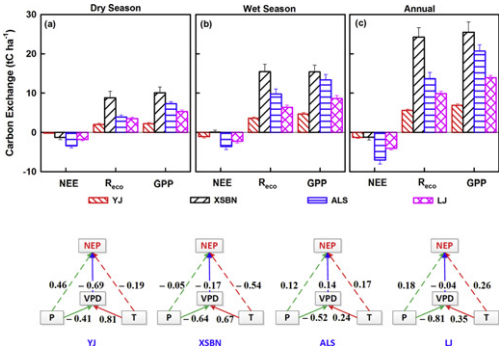

ARTICLE INFO

Article history:
Received 25 August 2017
Received in revised form 21 October 2017
Accepted 22 October 2017

Editor: Elena Paoletti

Keywords:
Carbon fluxes

ABSTRACT

Forest ecosystems play an increasingly important role in the global carbon cycle. However, knowledge on carbon exchanges, their spatio-temporal patterns, and the extent of the key controls that affect carbon fluxes is lacking. In this study, we employed 29-site-years of eddy covariance data to observe the state, spatio-temporal variations and climate sensitivity of carbon fluxes (gross primary productivity (GPP), ecosystem respiration (R_{eco}), and net ecosystem carbon exchange (NEE)) in four representative forest ecosystems in Yunnan. We found that 1) all four forest ecosystems were carbon sinks (the average NEE was -3.40 tC ha^{-1} yr^{-1}); 2) contrasting seasonality of the NEE among the ecosystems with a carbon sink mainly during the wet season in the Yuanjiang savanna ecosystem (YJ) but during the dry season in the Xishuangbanna tropical rainforest ecosystem (XSBN), besides an equivalent NEE uptake was observed during the wet/dry season in the Ailaoshan subtropical evergreen broad-

* Corresponding authors at: 88 Xuefu Road, Kunming, Yunnan 650223, PR China.
E-mail addresses: sqh@xtbg.ac.cn (Q. Song), yipingzh@xtbg.ac.cn (Y. Zhang).

https://doi.org/10.1016/j.scitotenv.2017.10.239
0048-9697/© 2017 Published by Elsevier B.V.

Critical factors
Path analysis
Redundancy analysis
Climate change
Forest ecosystems
Eddy covariance

leaved forest ecosystem (ALS) and Lijiang subalpine coniferous forest ecosystem (LJ); 3) as the GPP increased, the net ecosystem production (NEP) first increased and then decreased when the GPP > 17.5 tC ha^{-1} yr^{-1}; 4) the precipitation determines the carbon sinks in the savanna ecosystem (e.g., YJ), while temperature did so in the tropical forest ecosystem (e.g., XSBN); 5) overall, under the circumstances of warming and decreased precipitation, the carbon sink might decrease in the YJ but maybe increase in the ALS and LJ, while future strength of the sink in the XSBN is somewhat uncertain. However, based on the redundancy analysis, the temperature and precipitation combined together explained 39.7%, 32.2%, 25.3%, and 29.6% of the variations in the NEE in the YJ, XSBN, ALS and LJ, respectively, which indicates that considerable changes in the NEE could not be explained by variations in the temperature and precipitation. Therefore, the effects of other factors (e.g., CO_2 concentration, N/P deposition, aerosol and other variables) on the NEE still require extensive research and need to be considered seriously in carbon-cycle-models.

© 2017 Published by Elsevier B.V.

1. Introduction

Terrestrial ecosystems have a net carbon uptake from the atmosphere of 2.6 ± 1.2 Pg C yr^{-1} and therefore play a crucial role in the global carbon cycle by mitigating global warming (IPCC, 2013). A large portion of this uptake is absorbed by forest ecosystems, and the global spatio-temporal patterns of carbon exchange and their driving factors, especially in forest ecosystems, are the core of the global carbon cycle under climate change (Chapin et al., 2011; Heimann and Reichstein, 2008; IPCC, 2013; Le Quéré et al., 2016; Reichstein et al., 2013; Yu et al., 2014b). Therefore, exploring carbon exchanges and their responses to environmental factors is very important for understanding and projecting the carbon cycle and for providing information to policy-makers (Le Quéré et al., 2016). Such knowledge underpins the Paris Agreement, which aims to keep the rise in temperature well below 2 °C and calls for renewed efforts to limit global warming below 1.5 °C (Anderson and Peters, 2016; UNFCCC, 2015). So far, the most cost-effective approach to mitigate anthropogenic C emission is via ecosystem carbon uptake (IPCC, 2013). However, there remains a lack of knowledge on carbon fluxes and their spatio-temporal patterns, and the underlying mechanisms of critical factors impacting carbon fluxes.

The spatial representation of carbon fluxes is currently very limited and requires further comprehensive and cooperative research (Baldocchi, 2008; Yu et al., 2014b). Most recent studies have focused not only on the actualities of carbon exchange between forest ecosystems and the atmosphere, but also on the response of carbon fluxes to biophysical controls (Baldocchi et al., 2017; Beringer et al., 2016; Frank et al., 2015; Grace et al., 2014; IPCC, 2013; Reichstein et al., 2013; Yu et al., 2016). Many results showed that the decreased precipitation and increased temperature under climate change scenarios will decrease these ecosystems' carbon sinks (Chen et al., 2013; Ciais et al., 2005; Knapp et al., 2002; Weltzin et al., 2003; Wu et al., 2011), although a high degree of spatio-temporal heterogeneity exists, with marked influences from the topography, soil, vegetation and environmental factors in forest ecosystems (Baldocchi, 2008; Luyssaert et al., 2010; Luyssaert et al., 2008; Tagesson et al., 2016; Yu et al., 2014a; Yu et al., 2008). Undoubtedly, carbon exchanges and their controls differ between locations, with some ecosystems being especially vulnerable to climate change (Chen et al., 2013; IPCC, 2013; Jia et al., 2016; Mekonnen et al., 2016; Tagesson et al., 2016; Wu et al., 2011). Furthermore, biophysical-based models that predict the behavior of the global carbon cycle require much more knowledge derived from in situ research to drive and validate their results. National and global networks provide such data over time scales of years and even decades, and >900 observation stations were present in FLUXNET by the end of 2016 (http://fluxnet.fluxdata.org/sites/). Nevertheless, the spatio-temporal representativeness of flux recording is limited in many areas of the world (Pan et al., 2011; GR Yu et al., 2013a) despite attempts to improve our understanding of the global carbon exchange (Baldocchi, 2003; Baldocchi et al., 2001a; Baldocchi et al., 1996; Ciais et al., 2005; Falge et al., 2002; Law et al., 2002; Song et al., 2014; Yu et al., 2006; Zhang et al., 2010; Zhao et al., 2006). Clearly, we must comprehensively research carbon fluxes at a variety of scales (individuals, populations, communities, ecosystems, landscapes and regions) and infer their responses to climate change. Such studies should help to predict climate change, and the determined effects should also be helpful for regional carbon management to mitigate and adapt to climate change (Baldocchi, 2008; Wu et al., 2011; Yu et al., 2014b).

Southwest China has the second largest forest carbon biomass storage (Fang et al., 2001) and the largest carbon sink in China (Piao et al., 2009). However, this area is subject to climate change and may be vulnerable. Models suggested that Yunnan Province (the main portion of Southwest China) will experience decreased precipitation and increased temperatures (Gao et al., 2012; Qin et al., 2005). Therefore, it is imperative to understand the carbon exchanges and their responses to climate change in this region. An eddy covariance and meteorological observation system with long-term recording capability was applied at four contrasting forest ecosystems (YJ, XSBN, ALS, and LJ) along a large temperature and precipitation gradient in Yunnan to explore the carbon dynamics and their response to changing climate. The specific objectives of this study were to 1) quantify the carbon exchange state (gross primary productivity (GPP), ecosystem respiration (R_{eco}), and net ecosystem carbon exchange (NEE)) and its spatio-temporal patterns; 2) provide data to analyze the relationship among R_{eco}, NEE and GPP; 3) identify the influence of temperature (T) and precipitation (P) on the NEE, and 4) predict likely changes in carbon sinks under climate change. The over-arching aims are to predict the responses of forest ecosystems to climate change and thus contribute to the development and implementation of policies for regional ecosystem protection.

2. Materials and methods

2.1. Experimental sites

Four representative forest ecosystems, namely, the Yuanjiang savanna ecosystem (YJ), Xishuangbanna tropical rainforest ecosystem (XSBN), Ailaoshan subtropical evergreen broad-leaved forest ecosystem (ALS), and Lijiang subalpine cold-temperate coniferous forest ecosystem (LJ) (Fig. 1), were chosen to study the carbon exchanges and responses to climatic control in Yunnan, Southwest China.

The mean annual temperature over the study period (MAT) in the YJ, XSBN, ALS, and LJ was 24.3, 21.4, 11.7, and 7.9 °C, respectively, and the mean annual precipitation (MAP) was 734, 1415, 1728, and 1095 mm, respectively (Table 1). The climate is influenced by the southwestern monsoon and the Tibetan Plateau, and >80% of the MAP occurs during the wet season (May–October) in each of the four locations. The geographical location, altitude, dominant species, biophysical factors, and soil physical and chemical properties are listed in Table 1, and further information regarding the topography, climate, solar radiation, vegetation, and soil properties can be viewed in previous work (Cao et al.,

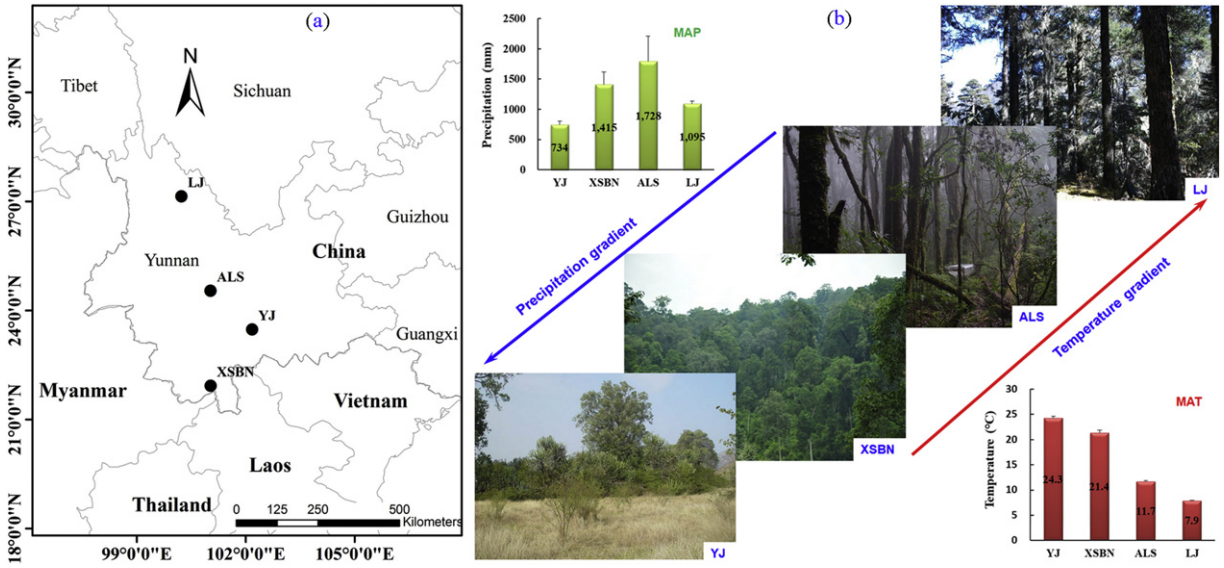

Fig. 1. Geophysical location (a) and overview (b) of the research ecosystems in Yunnan, Southwest China: Yuanjiang semi-arid savanna ecosystem (YJ, special terrain and vegetation), Xishuangbanna tropical rainforest ecosystem (XSBN, northern edge of the India-Malaysia tropical rainforest), Ailaoshan subtropical evergreen broad-leaved forest ecosystem (ALS, boundary of the East-South Asian monsoon area), and Lijiang subalpine cold-temperate coniferous forest ecosystem (LJ, extended regions of the Tibetan Plateau). All the studied ecosystems are indicated by circles.

Table 1
Overview of the forest ecosystems (YJ, XSBN, ALS, and LJ) that were studied in this research.

Variables	Research ecosystems			
	YJ	XSBN	ALS	LJ
Ecosystem type	Savanna ecosystem	Tropical rainforest ecosystem	Subtropical evergreen broad-leaved forest ecosystem	Subalpine coniferous forest ecosystem
Geographical location	23°28′26″ N, 102°10′39″ E	21°55′39″ N, 101°15′55″ E	24°32′17″ N, 101°01′45″ E	27°08′32″ N, 100°13′38″ E
Altitude (m)	550	750	2500	3240
MAT (°C)	24.3	21.4	11.7	7.9
MAP (mm)	734	1415	1728	1095
R/A ratio	81%	80%	81%	80%
SVWC in rainy season (%)	10–35	16–40	25–45	20–45
SVWC in dry season (%)	6–20	10–25	15–35	15–35
Soil type	Dry-red soil	Latosol	Yellow-brown soil	Dark-brown soil
Humus layer (cm)	–	~1[b]	7–12[b]	–
pH of the soil	7.3	4.5–5.5[b]	4.4–4.9[b]	5.6–5.9[d]
Organic carbon (g kg^{-1})	12.1	27.8[c]	138.4[c]	–
Total nitrogen (g kg^{-1})	1.0	2.8[c]	8.8[c]	4.0[e]
Total phosphorus (g kg^{-1})	0.30[a]	0.26[b]	0.82[b]	–
C/N ratio	12.1	9.9[b]	15.7[b]	–
Vegetation	Savanna	Tropical rainforest	Subtropical evergreen forest	Subalpine coniferous forest
Dominant species	*Lannea coromandelica*, *Polyalthia suberosa*, *Heteropogon contortus*	*Terminalia myriocarpa*, *Barringtonia pendula*, *Saprosma ternatum*, *Pteris cretica*	*Lithocarpus xylocarpus*, *Schima noronhae*, *Fargesia nitida*, *Plagiogyria communis*	*Picea likiangensis*, *Abies forrestii*, *Quercus guayavefolia*, *Acer pectinatum*, *Padus brachypoda*
Average canopy height (m)	4–6	35	25–30	38–42
LAI	~1.5	~5	~4.3	~3
Biomass (t ha^{-1})	~70[f]	>500[g]	~465.7[h]	–
Litterfall (t ha^{-1})	4.31[f]	9.91[g]	8.62[i]	5.11

Notes: MAT: mean annual temperature, MAP: mean annual precipitation, R/A ratio: ratio of the precipitation during the rainy season to the annual precipitation, and SVWC: soil volumetric water content. The references were cited from: a (Liu et al., 2007); b (Chan et al., 2006); c (Qiao et al., 2013); d (Qing, 2004); e (HX Yu et al., 2013b); f (Fei et al., 2017); g (Tan et al., 2010); h (Nizami et al., 2017); and i (Tan et al., 2011).

2006; Chan et al., 2006; Fei et al., 2016; Huang et al., 2017; Liu et al., 2007; Liu et al., 2002; Song et al., 2017; YP Zhang et al., 2006).

2.2. Eddy covariance and ancillary data

2.2.1. Flux and meteorological data

An open path eddy covariance (OPEC) system, which provides a direct, continuous and simultaneous measurement of scalar fluxes (e.g., energy, water and carbon fluxes) and environmental factors with a high time-resolution dataset between the ecosystem and atmosphere (Aubinet et al., 2001; Baldocchi et al., 2001a; Baldocchi et al., 1996), was applied to simultaneously measure the carbon fluxes and climatic variables in all four of the studied ecosystems (YJ, XSBN, ALS, and LJ) beginning in 2013, 2002, 2008, and 2014, respectively, to explore the carbon exchanges and their responses to critical climatic factors. The data that were used in this study spanned from May 2013 to 2016, 2003 to 2016, 2009 to 2016, and August 2014 to 2016 in the YJ, XSBN, ALS, and LJ, respectively. All the data in the tables and figures are multiyear averaged values.

The characteristics and parameters of the four sets of OPEC systems and routine meteorological instruments in this research (Table S1) are as follows: 1) the OPEC system consisted of a high-frequency (10 Hz) open-path CO_2/H_2O infrared gas analyzer and a tri-axial sonic anemometer; 2) a solar radiometer measured the global radiation (R_g); 3) a profile measurement system was employed to observe photosynthetically active radiation (PAR); 4) various instruments were installed to measure the relative humidity (RH) and air T (T_{air}) profiles; 5) the profiles of the soil moisture and soil T (T_{soil}) were measured; and 6) rainfall was measured by using a rain gauge at the top of each flux tower. More details regarding the OPEC systems and other meteorological instruments are provided in Table S1. The sampling frequencies of the flux and meteorological data were 10 Hz and 0.5 Hz, respectively. All the data were continuously collected by using Campbell loggers (CR1000/CR3000/CR5000, Campbell Scientific Inc., Logan, UT, USA) beginning in May 2013, October 2002, September 2008, and August 2014 in the YJ, XSBN, ALS and LJ, respectively.

2.2.2. LAI and litterfall

In each of our research ecosystems: 1) an LAI-2200 plant canopy analyzer (Li-Cor Inc., USA) was used to measure the monthly LAI at the end of each month (8 plots × 4 repeats) and data were processed with the FV2200 software (Li-Cor Inc., USA), and 2) 25 randomly distributed litterfall traps were used to capture the above-ground litterfall, which was collected on the last day of every month, sorted, dried (at 65 °C to a constant weight) and separated into components (leaves, branches, flowers, fruits, and others).

2.3. Data processing and statistical analysis

2.3.1. Data processing

Quality assessment and control (QA/QC) was applied according to the standard protocols that were recommended by several authors (Baldocchi et al., 2001a; Reichstein et al., 2005; Yu et al., 2006). FLUXNET, as well as ChinaFLUX, has developed a series of standard QA/QC methods to control and ensure the quality of flux data. For details regarding the flux data QA/QC and post-processing procedures in this study, see Reichstein et al. (2005) and Yu et al. (2006). Here, we briefly introduce the data processing flow: 1) three-dimensional/triple-coordinate rotation was applied to align the horizontal wind to the mean wind direction for instrument tilt or irregularities in the terrain effects on airflow (Baldocchi et al., 2000; Tanner and Thurtell, 1969; Wilczak et al., 2001; Zhu et al., 2005); 2) WPL calibration was used to correct flux data for air-density variations from the transfer of heat and water vapor (Lee and Massman, 2010; Webb et al., 1980); 3) the F_s value between the EC height and ground was calculated (Baldocchi et al., 1996; Carrara et al., 2003; Hollinger et al., 1994; Zha et al., 2004); 4) data that were collected during rainy periods were eliminated (Yu et al., 2006); 5) outliers were identified and rejected (Reichstein et al., 2005), and absolute NEE values > 50 μmol m^{-2} s^{-1} were discarded; 6) negative nighttime data were rejected; 7) a friction velocity (u*) threshold (0.2 in the YJ, ALS, and LJ and 0.12 in the XSBN) was applied to screen flux data (Falge et al., 2001; Reichstein et al., 2005; Saleska et al., 2003); and 8) marginal distribution sampling (Reichstein et al., 2005), which effectively combined the mean diurnal variation (MDV) and the look-up table method (Falge et al., 2001; Papale et al., 2006; Reichstein et al., 2005), was applied to fill in any gaps, and an online procedure that was recommended by FLUXNET and EUROFLUX (http://www.bgc-jena.mpg.de/~MDIwork/eddyproc/index.php) was used to partition the flux data.

2.3.2. Carbon exchange components and calculation

The Net Ecosystem Exchange (NEE) consists of two components, namely, the turbulent eddy flux (F_c) and the storage flux (F_s) (Aubinet et al., 2001; Baldocchi et al., 1996; Hollinger et al., 1994; Lee et al., 2006), as expressed in Eq. (1):

$$NEE = F_c + F_s = \rho\overline{w'c'} + \frac{\Delta c}{\Delta t} z_r \quad (1)$$

where F_c represents the turbulent eddy flux that is transported above the EC system height (13.9, 48.8, 34, and 60 m in the YJ, XSBN, ALS, and LJ, respectively) and the atmosphere, and F_s indicates the storage flux under the plane of the EC system and ground surface. A single-point (i.e., EC) method was applied to measure F_s at the measurement height (z_r) of the fluxes; ρ, w, and c represent the air density, vertical wind velocity, and target scalar concentration (CO_2 concentration in this case), respectively; the primes denote fluctuations from the average; and the overbar signifies a time average (30 min in this case). Δc is the variation over a 30-min period at height z_r, z_r is the height of the EC system, and Δt is the time interval (1800 s in this case). By convention, NEE equals the negative net ecosystem productivity (NEP). A negative NEE (or positive NEP) indicates that the ecosystem acts as a carbon sink and fixes carbon from the atmosphere, i.e., photosynthesis exceeds all respiratory losses.

The ecosystem respiration (R_{eco}) and gross primary productivity (GPP) can be derived from the eddy flux (Baldocchi et al., 2001a; Gilmanov et al., 2007; Reichstein et al., 2005; Yu et al., 2006) as expressed in Eqs. (2) and (3):

$$R_{eco} = R_{eco,ref} \times e^{E_0 \left(\frac{1}{T_{ref}-T_0} - \frac{1}{T-T_0}\right)} \quad (2)$$

$$GPP = R_{eco} + (-NEE) \quad (3)$$

where R_{eco} is the ecosystem respiration after Lloyd and Taylor (1994); $R_{eco,\ ref}$ is the reference ecosystem respiration at the reference temperature (T_{ref}, here 10 °C); $R_{eco,\ ref}$, and E_0 are the fitted parameters; T_0 is a constant and set to 227.13 K (−46.02 °C); and T is the measured 5-cm soil temperature in this study. The units of T_0, T_{ref}, and T in Eq. (2) are in Kelvin. We followed the convention to express the absolute values of NEE and NEP, the gross ecosystem carbon exchange (GEE) and the GPP (i.e., NEP = −NEE, GPP = −GEE) (Baldocchi et al., 2001b; Falge et al., 2001; Goulden et al., 1996), although some authors noted that these variables do not necessarily represent the same quantity (Chapin et al., 2006; Randerson et al., 2002).

2.4. Statistical analysis

The intra-annual and seasonal variations in the meteorological data and carbon exchanges were analyzed. In addition, the coefficient of variation (CV) was analyzed to quantify the variation in the inter-annual carbon exchange. Then, path analysis was applied to suggest the direct and total effects of T, P and their comprehensive expression

(e.g., vapor pressure deficit, VPD) on the NEP at a monthly timescale. We then used redundancy analysis (RDA) to determine the contributions from critical climatic factors to the NEE. Finally, regression analysis was performed to quantify the responses of the carbon exchange (GPP, R_{eco}, and NEE) to "the critical climatic factors (T and P)" according to the results of RDA at a daily timescale. The details of the data analysis are as follows.

2.4.1. Path analysis

Path analysis was first proposed by Sewall Wright, a quantitative geneticist, in 1921 (Wright, 1921). It is based on the fundamental principles of multiple regression and correlation analysis but has a more interpretive structure (Grace and Bollen, 2005). In addition, this method is an especially useful analytic tool when the relationships (a priori causal connections) among variables are well known (Li, 1975; Schemske and Horvitz, 1988). Path analysis shows us not only the direct effects of independent factors on dependent variables but also the indirect and total effects (total effects = direct effects + indirect effects) (Chen et al., 2015; Li, 1975; Schemske and Horvitz, 1988; Wootton, 1994). In addition, path analysis has been recently applied to explore the effects of biophysical controls on ecosystem carbon exchange and/or ET (Bassow and Bazzaz, 1998; Chen et al., 2015; Huxman et al., 2003; Olivas et al., 2010; Saito et al., 2009; Ueyama et al., 2014; Wu et al., 2017; Zhuang et al., 2016).

Here, we assume that the NEP was mainly controlled by T, P, and VPD at a monthly timescale because of the critical roles of T, P, and VPD in regulating carbon exchange (Baldocchi, 2008; Chen et al., 2013; Jung et al., 2017; Reichstein et al., 2007; GR Yu et al., 2013a). Then, path analysis was applied to statistically identify which climatic drivers significantly influenced the NEE and quantify their relative importance through parameterizing the standardized direct and total effects on the NEP. We first designed the path structure for the correlations of P, T, and VPD with the NEP as follows: 1) T and P directly and indirectly and determine the NEP; 2) T and P jointly drive VPD; and 3) VPD directly affects the NEP. In this study, our purpose was not to explore the relative goodness of fit between different path structures, although other path-structure models may be more feasible, but instead to identify the quantitative importance of climatic factors (T, P, and VPD) on the carbon sink. The R package *sem* (Fox et al., 2016) was used to conduct path analysis, and the path coefficients (PCs) were standardized partial regression coefficients, representing the relative strength of a given relationship, and allowed us to quantitatively compare the relative influence of T, P, and VPD on the NEP.

2.4.2. Redundancy analysis to quantify the contributions

RDA provides a useful statistical method to identify the critical controls and determine the further effect size for each defined critical biophysical factor by parsing out other factors as given constraints to calculate its total explanatory power (De'ath and Fabricius, 2000; Oksanen, 2015). This method was applied to quantify the contributions of critical explanatory variables (T and P) to the response variables (e.g., NEE), as the NEE is mainly controlled by T and P (Anderson-Teixeira et al., 2011; Jung et al., 2017; Yu et al., 2010). In this study, the R software and *vegan* R package were used to calculate the RDA (Oksanen, 2015) at a monthly time scale.

2.4.3. Regression analysis

The one-factor quadratic/exponential regression and two-factor regression models were used to quantify the relationship of T_{air} and the soil volumetric water content (SVWC) with the carbon exchange (GPP, R_{eco}, and NEE) at daily timescales as follows (Reichstein et al., 2002; Wen et al., 2010; Yu et al., 2004):

$$f(x) = ax^2 + bx + c \tag{4}$$

$$R_{eco} = a \times \exp(bT) \tag{5}$$

$$f(x) = a \times \exp(bT) \times W^c \tag{6}$$

The exponential model (Eq. (5)) was used to explore the effect of T_{air} on R_{eco}, and the quadratic regression model (Eq. (4)) was used to study the responses of 1) the GPP, R_{eco}, and NEE to SVWC and 2) the GPP and NEE to T_{air}. Additionally, the two-factor regression model (Eq. (6)) was applied to explore the interactive effect of T_{air} and SVWC on the GPP, R_{eco}, and NEE. In Eqs. (4)–(6), where a, b, and c are fitted parameters, x represents T_{air} or SVWC; $f(x)$ represents the GPP, R_{eco}, or NEE; and T and W represent T_{air} and SVWC, respectively.

3. Results

3.1. Spatiotemporal variation in carbon exchange

3.1.1. Seasonally and yearly binned mean diurnal variations in carbon exchange

Generally, the diurnal patterns of the NEP (NEP = −NEE) were consistent with those of the GPP, increasing with higher solar elevation (elevation angle of the Sun) in the four studied forest ecosystems (YJ, XSBN, ALS, and LJ), and the half-hourly GPP and NEP peaked at midday (12:00–13:00) and then decreased with decreasing solar elevation (Fig. 2). In contrast, the minimum R_{eco} occurred before sunrise, after which this value gradually increased and peaked late in the afternoon at 16:00. These dynamics were very clear, especially in the XSBN. Interestingly, the GPP and carbon-sink strength (absolute NEE values) peaked at 12:00 in the YJ (Fig. 2a1, b1, c1) and XSBN (Fig. 2a2, b2, c2), but the time of the GPP and NEE peak in the ALS (Fig. 2a3, b3, c3) and LJ (Fig. 2a4, b4, c4), where T was lower and the soil water was higher than in the YJ and XSBN (Table 1), was delayed by approximately 1–1.5 h compared to the peak time in the YJ and XSBN.

For each ecosystem, the GPP, R_{eco}, and NEE during the wet season (May–October) were higher than those during the dry season (November–April) (Fig. 2). The diurnal magnitude of the GPP, R_{eco}, and NEE showed trends of XSBN > ALS > LJ > YJ, and higher GPP produced higher R_{eco} within the same ecosystem, suggesting that the photosynthetic capacity controlled R_{eco}.

3.1.2. Intra-annual variations in meteorological conditions and carbon exchanges

3.1.2.1. Intra-annual variations in meteorological conditions. The detailed intra-annual analysis of the meteorological conditions in the four forest ecosystems (Fig. 3) showed clearly that 1) the R_g and PAR peaked from April to May in all cases (YJ, XSBN, ALS, and LJ) and that the dynamics of the PAR were consistent with those of R_g, although the R_g and PAR changed more dramatically in the wet season in the ALS and LJ than in the YJ (Fig. 3a, e); 2) the dynamics of T_{air} and T_{soil} were highly coincident: the lowest T_{air} and T_{soil} occurred at the end of December to the middle of January, and the highest T_{air} and T_{soil} occurred from May to June in the YJ, in contrast to the peaks occurring approximately one month later (in July) in the XSBN, ALS, and LJ (Fig. 3b); 3) the multi-annual mean VPD was 13.7, 6.3, 3.4, and 3.6 hPa in the YJ, XSBN, ALS, and LJ, respectively (Fig. 3c), the daily VPD dramatically changed in the YJ and peaked from April to May, and the RH dynamics contrasted those of VPD; and 4) the SVWC at −5 cm and −40 cm consistently changed in the four ecosystems, with the lowest SVWC occurring at the end of the dry season (April) and the SVWC being higher during the wet season (Fig. 3d), reflecting the fact that almost 80% of the precipitation fell during the rainy season (Fig. 3e and Table 1).

3.1.2.2. Intra-annual variation in carbon exchanges. Generally, photosynthesis was more efficient and showed higher GPP (GPP = −GEE) during the wet season (May–October) than the dry season (November–April) in the YJ, XSBN, ALS and LJ, and the total R_{eco} was higher during

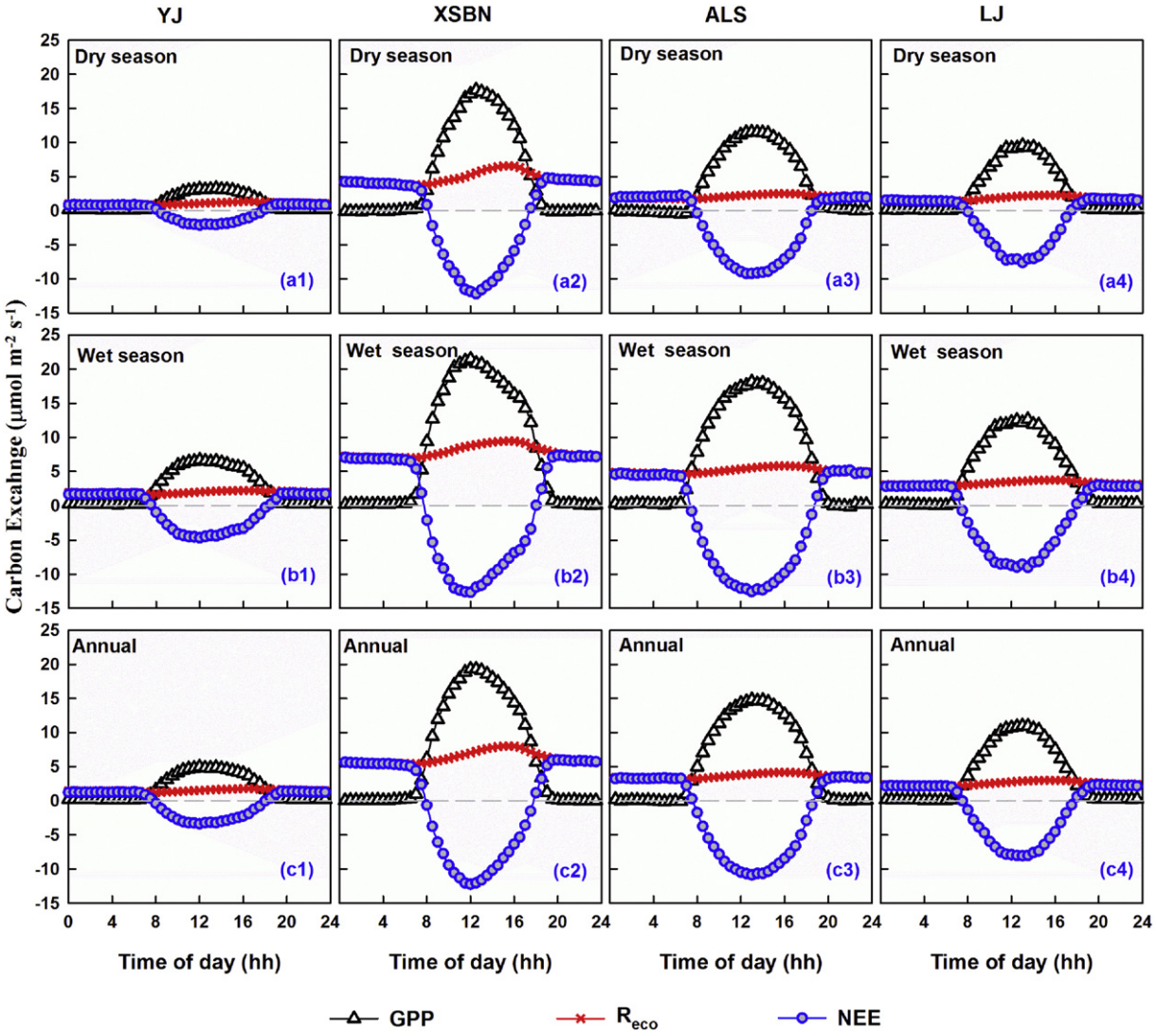

Fig. 2. Mean diurnal variations in the dry season-binned (a1–a4), wet season-binned (b1–b4), and annual-binned (c1–c4) gross primary productivity (GPP), ecosystem respiration (R_{eco}), and net ecosystem carbon exchange (NEE) in the Yuanjiang semi-arid savanna ecosystem (YJ), Xishuangbanna tropical rainforest ecosystem (XSBN), Ailaoshan subtropical evergreen broad-leaved forest ecosystem (ALS) and Lijiang subalpine coniferous forest ecosystem (LJ) in Yunnan Province, Southwest China.

the wet season than the dry season (Fig. 4). For example, the highest GPP and R_{eco} (almost 12 g C m^{-1} day^{-1}) occurred in the XSBN and ALS in August, and the GPP and R_{eco} were usually correlated. The GPP and R_{eco} ranked as follows: XSBN > ALS > LJ > YJ. The GPP in the XSBN was very high compared to the GPP in the YJ, and the lowest GPP and R_{eco} in the XSBN (usually in December or January) approached the highest GPP and R_{eco} in the YJ (Fig. 4a, b), which indicated that precipitation restricted photosynthesis in the YJ. In summary, the photosynthetic capacity and R_{eco} of the tropical rainforest (e.g., XSBN) and subtropical evergreen broad-leaved forest (e.g., ALS) were more efficient than those of savanna vegetation.

A net carbon sink was observed almost daily in the ALS and LJ (Fig. 4c, d), whereas the carbon sink in the YJ mainly occurred from June to November (with a peak in August) (Fig. 4a) and showed an opposite pattern in the XSBN, in which carbon sequestration mainly occurred from the late wet season to the middle of the dry season (September–March) (Fig. 4b).

3.1.3. Seasonal and annual dynamics of the meteorological conditions and carbon exchanges

3.1.3.1. Seasonal and annual dynamics of the meteorological conditions. To sum up, R_g, PAR, P, T_{air}, T_{soil}, RH, and SVWC were higher during the wet season than the dry season, except for the R_g and PAR in the ALS and LJ (Table 2). Usually, the VPD, as in the XSBN, ALS, and LJ, was larger during the dry season than the wet season because >80% of the annual precipitation occurred during the wet season. However, the VPD showed the opposite seasonal trend in the YJ, measuring 15.2 hPa during the wet season and 12.1 hPa during the dry season (Table 2) due to a lack of rain but abundant radiation.

3.1.3.2. Seasonal and annual dynamics of the carbon exchanges. Seasonally, the GPP and R_{eco} (i.e., carbon intake and output) during the wet season were higher than those during the dry season: the GPP was 4.69 ± 0.37, 15.38 ± 1.73, 13.37 ± 1.39, and 8.62 ± 0.77 tC ha^{-1} during the wet season and 2.21 ± 0.31, 10.09 ± 1.47, 7.31 ± 0.47, and 5.30 ± 0.42 tC ha^{-1} during the dry season, and R_{eco} was 3.61 ± 0.34, 15.43 ± 1.90, 9.76 ± 1.28, and 6.37 ± 0.57 tC ha^{-1} during the wet season and 2.01 ± 0.31, 8.79 ± 1.67, 3.90 ± 0.54, and 3.50 ± 0.35 tC ha^{-1} during the dry season in the YJ, XSBN, ALS, and LJ, respectively. Therefore, the YJ, ALS, and LJ were carbon sinks not only during the wet season (−1.08 ± 0.35, −3.61 ± 0.77, and −2.24 ± 0.51 tC ha^{-1}, respectively) but also during the dry season (−0.20 ± 0.09, −3.41 ± 0.56, and −1.81 ± 0.28 tC ha^{-1}, respectively) (Fig. 5a, b). An unusual seasonal

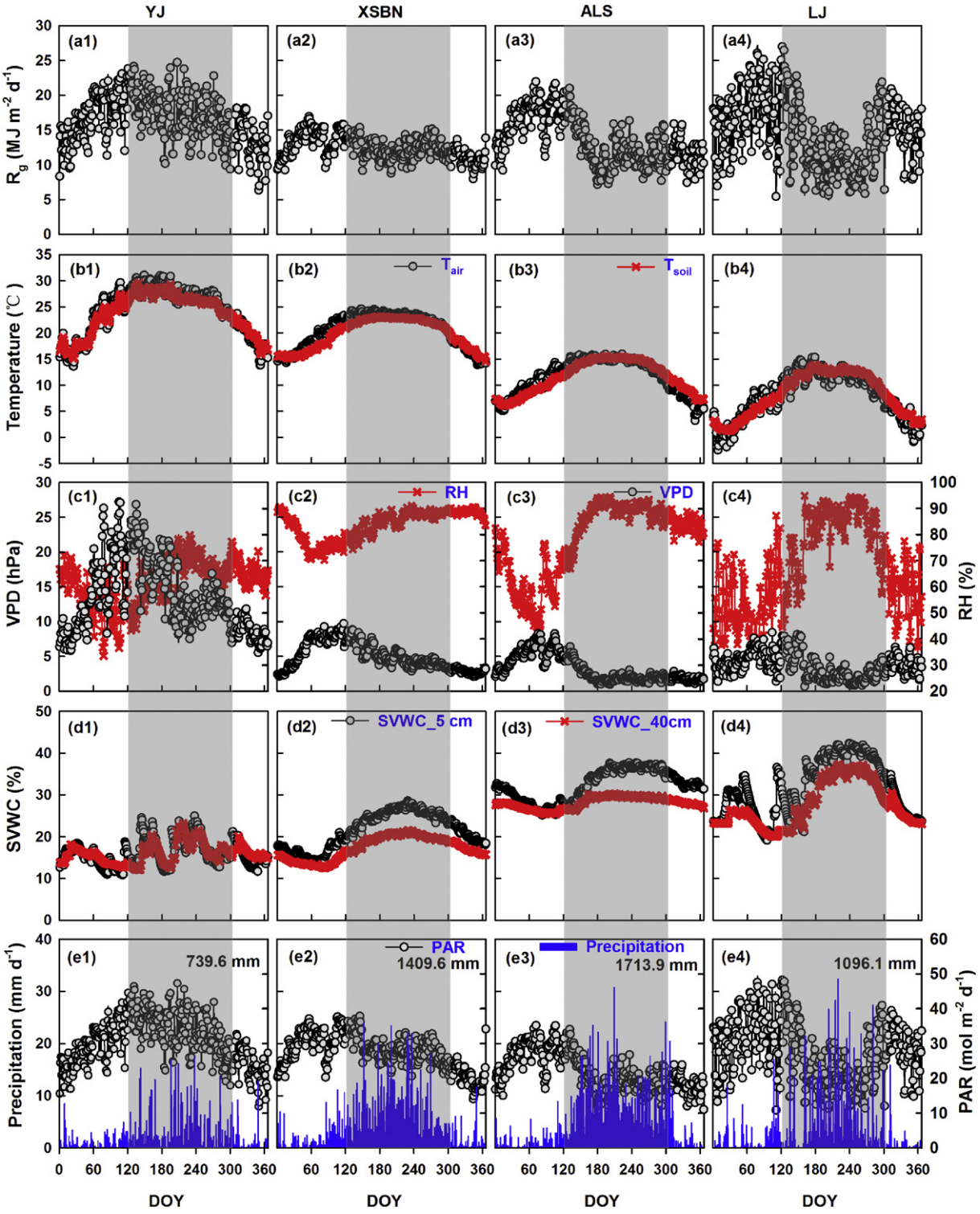

Fig. 3. Seasonal and annual patterns of the averaged multiyear meteorological factors in the Yuanjiang semi-arid savanna ecosystem (YJ), Xishuangbanna tropical rainforest ecosystem (XSBN), Ailaoshan subtropical evergreen broad-leaved forest ecosystem (ALS) and Lijiang subalpine coniferous forest ecosystem (LJ) in Yunnan Province, Southwest China: (a) daily summed global radiation (R_g) above the canopy; (b) average daily air temperature (T_{air}) and soil temperature (T_{soil}) at −5 cm; (c) averaged daily relative humidity (RH) and saturation vapor pressure deficit (VPD); (d) soil volumetric water content (SVWC) at −5 cm and −40 cm; and (e) daily summed photosynthetically active radiation (PAR) and daily summed precipitation. R_g, T_{air}, VPD, SVWC_5 cm, and PAR are represented by gray-filled black circles or lines; and T_{soil}, RH, and SVWC_40 cm are indicated with crossing solid lines. The rainfall is represented by blue-filled rectangles. The shaded areas indicate the wet season (May–October), and the rest represents the dry season (November–April). The available data periods in the YJ, XSBN, ALS, and LJ were May 2013 to 2016, 2003 to 2016, 2009 to 2016, and August 2014 to 2016, respectively.

pattern was present in the XSBN, in which a carbon sink mainly occurred during the dry season (−1.31 ± 0.56 tC ha^{-1}) but with a slight/marginal carbon source during the wet season (0.06 ± 0.51 tC ha^{-1}). The seasonality of the NEE was unremarkable in the ALS and LJ, which absorbed and fixed CO_2 nearly all year, whereas dramatic seasonal variations in the NEE were observed in the YJ and XSBN.

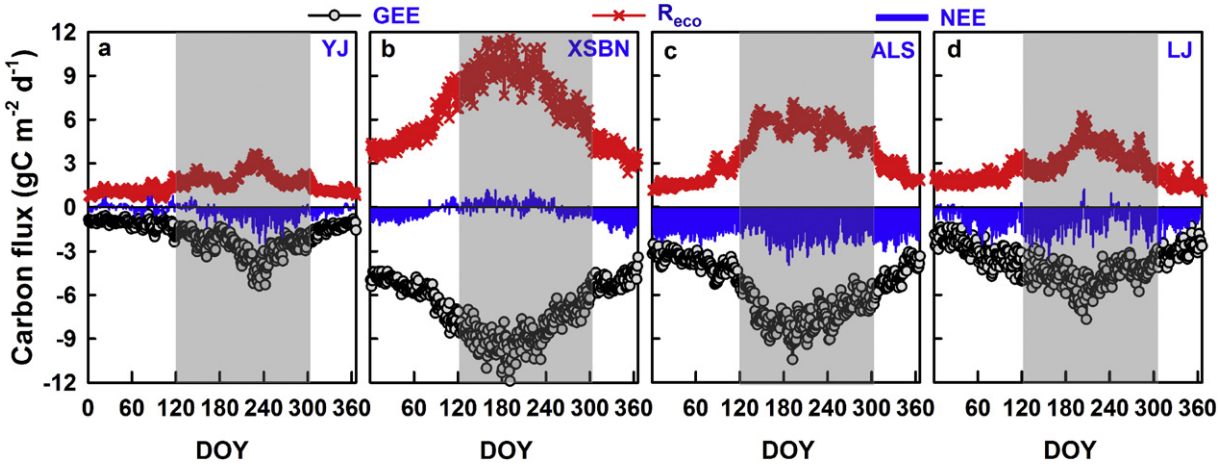

Fig. 4. Seasonal and annual patterns of the averaged multiyear gross ecosystem carbon exchange (GEE, GEE = −GPP; by convention, GEE is opposite in sign to GPP), total ecosystem respiration (R_{eco}), and net ecosystem carbon exchange (NEE) in the Yuanjiang semi-arid savanna ecosystem (YJ), Xishuangbanna tropical rainforest ecosystem (XSBN), Ailaoshan subtropical evergreen broad-leaved forest ecosystem (ALS) and Lijiang subalpine coniferous forest ecosystem (LJ) in Yunnan Province, Southwest China. The GEE is represented by gray-filled circles or lines, R_{eco} is indicated with crossing solid lines, and the NEE is represented by blue-filled rectangles. The shaded areas indicate the wet season, and the rest is the dry season.

Nearly 84% of the NEE was achieved during the wet season in the YJ, with the opposite seasonality occurring in the XSBN.

Annually, the YJ, XSBN, ALS, and LJ were carbon sinks: the NEE values were −1.28 ± 0.27, −1.25 ± 0.68, −7.02 ± 1.05, and −4.05 ± 0.41 tC ha^{-1} yr^{-1}, respectively (Fig. 5). The carbon-sink capability in the XSBN was nearly equivalent to that in the YJ, although the XSBN was the most efficient in terms of photosynthesis and had the highest GPP among our research ecosystems, while the highest R_{eco} occurred during the wet/dry season. In addition, the ALS showed the strongest carbon sink.

3.1.4. Relationship between the R_{eco} and NEP with the GPP

We used linear and quadratic regression models to explore the spatial (i.e., between-site) relationship between the R_{eco} and NEP with the GPP (Fig. 6). In addition, the spatial variations in R_{eco} were highly correlated to the spatial variations in the GPP in both types of models ($P < 0.001$), but the quadratic regression equation showed a higher R^2 ($R^2 = 0.94$). In contrast, only the quadratic regression model showed significance ($P = 0.0026$) in the relationship between the spatial variations in the NEP and GPP, and the NEP increased with the GPP when the GPP < 17.5 tC ha^{-1} yr^{-1}; otherwise, the NEP was negatively correlated to the GPP (Fig. 6b). The spatial variations in the GPP contributed 93.5% and 40.9% to the spatial variations in the R_{eco} and NEP, respectively, according to the quadratic regression equations (Fig. 6).

Table 2
Seasonal and annual variations in the meteorological conditions in the YJ, XSBN, ALS, and LJ.

Sites	Period	Seasonal or annual sum		Seasonal or annual average					
		R_g	PAR	P	T_{air}	T_{soil}	RH	SWVC	VPD
		MJ m^{-2} yr^{-1}	mol m^{-2} yr^{-1}	mm	°C	°C	%	%	hPa
YJ	DS	2918.7	5132.3	140.2	21.1	20.9	58.9	14.2	12.1
	WS	3230.2	6337.5	593.6	27.7	26.8	63.4	16.6	15.2
	A	6148.9	11,469.7	733.8	24.4	23.8	61.1	15.4	13.7
	WS/A	**0.53**	**0.55**	**0.81**	**1.14**	**1.12**	**1.04**	**1.08**	**1.11**
XSBN	DS	2515.4	5150.2	288.6	18.8	17.9	75.9	17.8	6.6
	WS	2647.4	5153.4	1124.9	24.0	23.1	82.4	23.4	6.0
	A	5162.9	10,303.6	1413.5	21.4	20.5	79.1	20.6	6.3
	WS/A	**0.51**	**0.50**	**0.80**	**1.12**	**1.13**	**1.04**	**1.14**	**0.96**
ALS	DS	2767.8	5077.3	331.5	9.0	8.7	66.9	30.2	4.4
	WS	2261.7	4290.2	1396.3	14.3	14.2	86.9	34.5	2.4
	A	5029.5	9367.6	1727.8	11.7	11.4	76.9	32.3	3.4
	WS/A	**0.45**	**0.46**	**0.81**	**1.22**	**1.24**	**1.13**	**1.07**	**0.70**
LJ	DS	2852.8	5595.7	219.5	4.2	4.6	54.9	26.8	4.2
	WS	2345.8	4438.1	875.8	11.5	12.0	80.3	33.9	3.0
	A	5198.6	10,033.7	1095.1	7.9	8.3	67.7	30.4	3.6
	WS/A	**0.45**	**0.44**	**0.80**	**1.46**	**1.45**	**1.18**	**1.12**	**0.83**

DS represents the dry season, WS represents the wet season, A means "annual", and WS/A is the ratio of the wet-season to the annual values.

3.2. Influences of critical climatic factors (T, P, and VPD) on the carbon sinks

Path analysis was used to further investigate how critical climatic factors (T, P, and VPD) influenced the NEP at a monthly scale. The results showed that the monthly variations in the NEP were jointly controlled by variations in T, P, and VPD, although with different path coefficients in the YJ, XSBN, ALS, and LJ (Fig. 7).

Overall, the monthly variations in P controlled the monthly variations in the NEP with direct effects of 0.18, −0.20, 0.19, and 0.15 in the YJ, XSBN, ALS, and LJ, respectively, and total effects of 0.46, −0.09, 0.12, and 0.18 in the YJ, XSBN, ALS, and LJ, respectively (Fig. 7). In addition, the monthly variations in T controlled the monthly variations in the NEP, with direct effects of 0.37, −0.41, 0.13, and 0.27 in the YJ, XSBN, ALS, and LJ, respectively, and total effects of −0.19, −0.54, 0.17, and 0.26 in the YJ, XSBN, ALS, and LJ, respectively (Fig. 7). In addition, the direct effects of VPD on the NEP were negative in the YJ (−0.69) and XSBN (−0.17) but positive in the ALS (0.24), suggesting that the VPD was the dominant controller of the carbon sink in the YJ and was not a constraining factor in the ALS. The results suggested that the VPD (comprehensive expression of the contradiction between water and energy/T) and P were the critical controls and exhibited a dominant effect on the carbon sink in the YJ, while T was the main factor in the XSBN, ALS and LJ. T had a strong negative effect on the NEP in the XSBN.

3.3. Quantifying the contributions from temperature and precipitation to the NEE

The RDA results showed that T and P jointly explained 39.7%, 32.2%, 25.3%, and 29.6%, T explained 3.1%, 13.8%, 10.1%, and 11.7%, and P explained 15.3%, 2.9%, 8.5%, and 10.4% of the variations in the NEE in the YJ, XSBN, ALS and LJ, respectively (Fig. 8). T and P jointly explained >1/3 (39.7%) of the variations in the NEE in the YJ and nearly 1/3 (32.2%) in the XSBN, which indicated that the carbon sinks (NEE) in the YJ and XSBN were more easily affected by T and P than in the ALS and LJ, while the NEE in the ALS and LJ were jointly determined by T

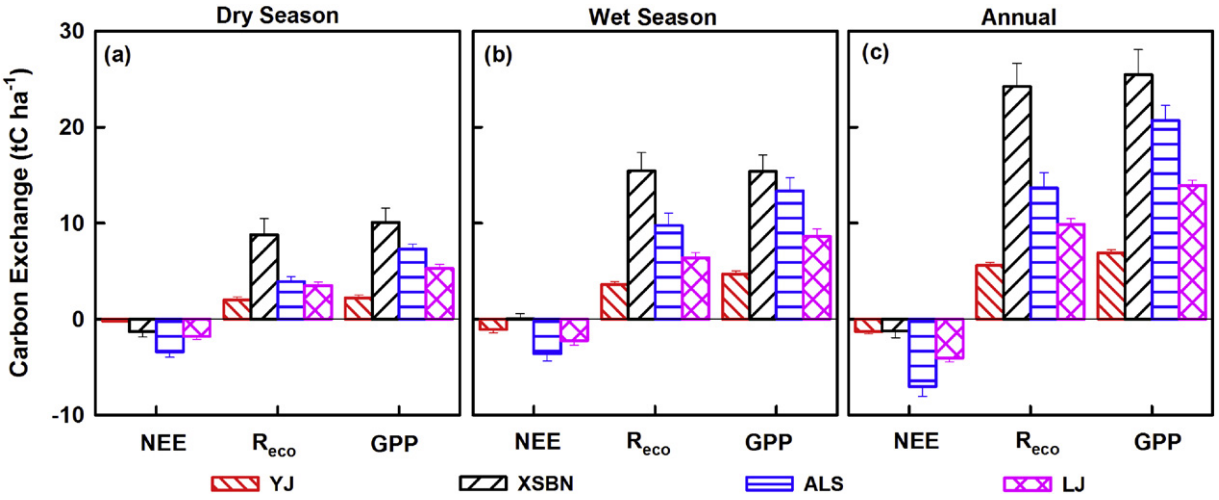

Fig. 5. Carbon exchange (NEE, R_{eco}, and GPP) variations during the dry season (a), wet season (b) and annual period (c) in the Yuanjiang semi-arid savanna ecosystem (YJ), Xishuangbanna tropical rainforest ecosystem (XSBN), Ailaoshan subtropical evergreen broad-leaved forest ecosystem (ALS) and Lijiang subalpine coniferous forest ecosystem (LJ) in Yunnan Province, Southwest China. The error bar indicates the standard deviation (sd).

and P (Fig. 8). Furthermore, the overlapping areas of T and P in the YJ and XSBN (21.3% and 15.5%) were larger than those in the ALS and LJ, which suggested a strong interaction between P and T in the YJ and XSBN. Overall, the variation in the NEE in the YJ and XSBN was mainly controlled by P and T, respectively, which are readily affected under climate change (warming/drought). Additionally, the RAD results demonstrated that T and P were the critical controls of the NEE in these ecosystems. Therefore, the responses of carbon exchange to T and P will be analyzed next.

3.4. Responses of carbon exchanges to temperature and precipitation

3.4.1. Responses of carbon exchanges to temperature

The one-factor quadratic and exponential models (Eqs. (4) and (6)) were applied to quantify the relationship of T_{air} with the GPP, R_{eco}, and NEE (Fig. 9). In addition, just as the regression results showed that the GPP decreased with increasing T_{air} in the YJ but increased in the XSBN, ALS, and LJ, and R_{eco} increased with increasing T_{air} in all the studied forest ecosystems, which resulted in a decreased carbon sink (lower absolute values of NEE) in the YJ with increasing T_{air} for increasing R_{eco} and decreasing GPP (Fig. 9a). However, R_{eco} showed higher T sensitivity than the GPP in the XSBN, and these variations resulted in a significantly decreased carbon sink with *P* values at the 0.001 level (Fig. 9a). In the ALS and LJ, the carbon sink, therefore, may have strengthened because the MAT (11.7 °C and 7.9 °C in ALS and LJ, respectively) was relatively lower, and the T sensitivity of the GPP and R_{eco} was nearly at the same level/velocity (Fig. 9c, d). In summary, future warming may be expected to reduce the carbon sinks in warmer regions (e.g., in the YJ and XSBN, where the MAT was 24.3 °C and 21.4 °C, respectively) but may enhance photosynthesis and increase the carbon sinks in relatively cool regions (e.g., the ALS and LJ) in Yunnan, Southwest, China.

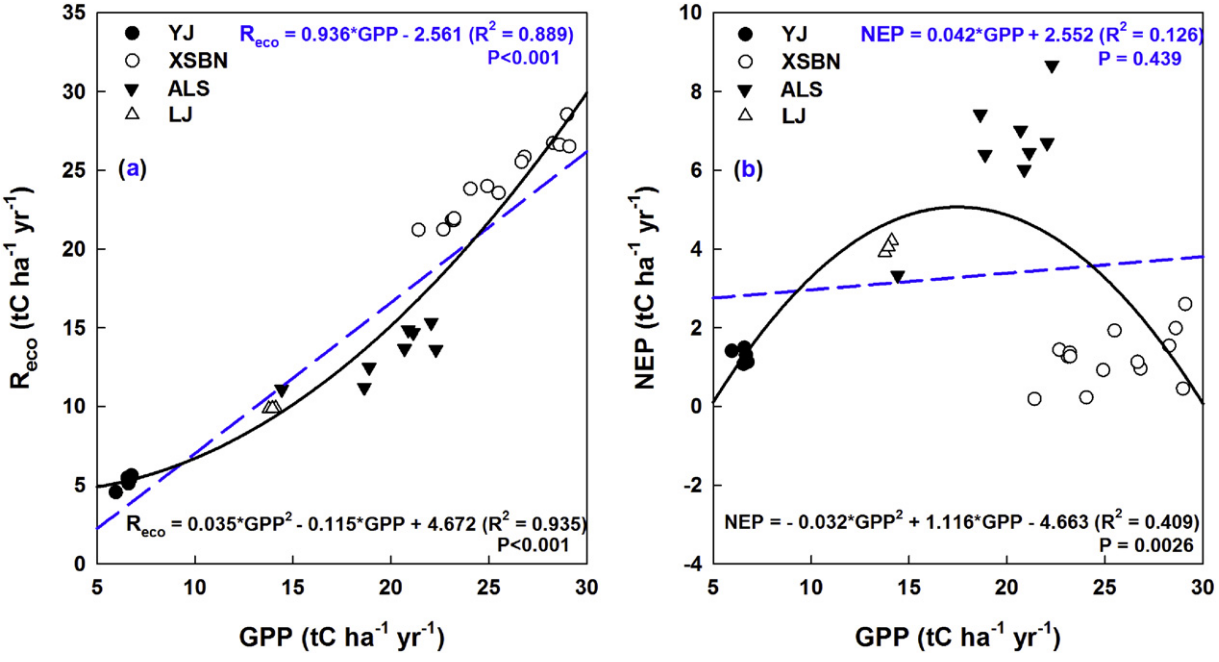

Fig. 6. Coupled relationships between the annual R_{eco} and NEP with the annual GPP in YJ, XSBN, ALS, and LJ in Yunnan Province, Southwest China.

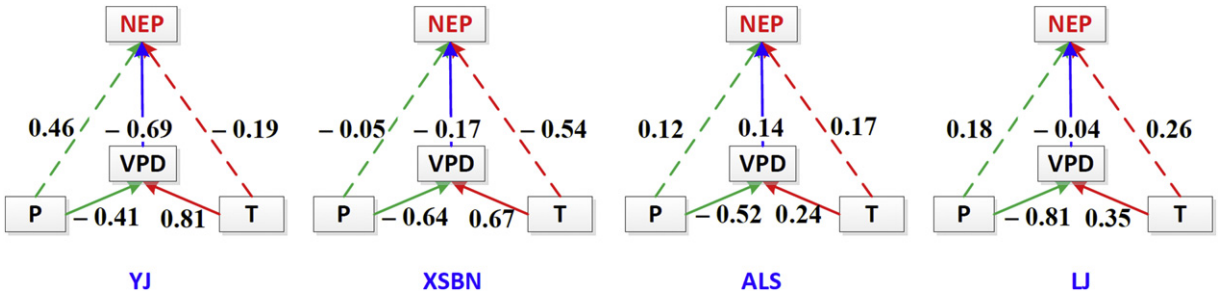

Fig. 7. Schematic diagrams that illustrate the effects of climatic controls on the monthly variations in the NEP in Yunnan's typical forest ecosystems (YJ, XSBN, ALS, and LJ). The solid arrows are the direct effects (standardized partial-regression coefficient), and the dashed arrows indicate the total effects (total effects = direct effects + indirect effects). The values that neighbor the solid and dashed arrows represent the direct path coefficient and total path coefficient, respectively. "NEP" is the net ecosystem productivity (NEP = −NEE). T, P, and VPD indicate the mean monthly T, monthly precipitation, and mean monthly vapor pressure deficit, respectively.

The temperature sensitivity (assessed as Q_{10}) of R_{eco} in the YJ, XSBN, ALS, and LJ was 1.49, 3.19, 4.19, and 2.37, respectively (Fig. 9). This result suggests that the R_{eco} values in the XSBN and ALS were more susceptible to any rise in temperature than those in the YJ and LJ.

3.4.2. Responses of carbon exchanges to soil volumetric water content

Both the GPP and R_{eco} decreased with decreasing SVWC in these ecosystems according to the one-factor quadratic and exponential regression results. The decreased SVWC (P) had little effect on the NEE and may have enhanced the carbon sinks in the XSBN, ALS, and LJ but had a significantly negative effect on the NEE in the YJ and weakened the carbon sink in this ecosystem (Fig. 10).

3.4.3. Interactive effects of the temperature and soil volumetric water content on the carbon exchanges in Yunnan's typical forest ecosystems

A two-factor regression model (Eq. (5)) was applied to explore the responses of the GPP, R_{eco}, and NEE to T_{air} and SVWC. The results showed that the GPP and R_{eco} generally increased with increasing T_{air} and SVWC (Fig. 11). However, the trend and extent of the NEE's responses to T and water were inconsistent. SVWC had more powerful influences on the NEE than T in the YJ, whereas the opposite occurred in the XSBN. On the other hand, T and SVWC had less influence on the NEE, especially in the ALS. Overall, the carbon sink sharply changed in the XSBN and YJ, more so than in the ALS and LJ under the joint effect of increased T and varying SVWC (Fig. 11).

4. Discussion

4.1. Carbon exchanges and their spatio-temporal variability

The carbon exchange in forest ecosystems often shows high spatial variability because of the interactions among environmental factors, topography and soil conditions (Pan et al., 2011; Piao et al., 2009; Yu et al., 2014a; GR Yu et al., 2013a). Strong spatial variability in the NEE was observed in this study (−1.28, −1.25, −7.02, and −4.05 tC ha^{-1} yr^{-1} in the YJ, XSBN, ALS, and LJ, respectively) (Fig. 5): the highest carbon sink occurred in the ALS, and the lowest occurred in the tropical rainforest ecosystem (XSBN), although this area had the highest GPP and R_{eco} (Fig. 5).

The strongest carbon sink (7.02 tC ha^{-1} yr^{-1}) occurred in the evergreen broadleaved old growth forest (ALS), which was entirely consistent with the biometric measurements within the same forest (~6 tC ha^{-1} yr^{-1}) from 2003–2007 (Tan et al., 2011) and 6.6 tC ha^{-1} yr^{-1} from 2005–2010 (Nizami et al., 2017). Although this area is considered to be 'old growth forest', it is still strongly absorbing carbon. It is now understood that old forests often act as carbon sinks, in contrast to the classical view that they reach an equilibrium state (Luyssaert et al., 2008). A strong carbon sink was also found in a subtropical evergreen conifer forest ecosystem in Florida (the multi-year mean NEE was −6.7 tC ha^{-1} yr^{-1}) (Bracho et al., 2012). Additionally, an interesting intra-annual pattern indicated that each month showed a carbon sink in the ALS and LJ (Fig. 4); similar results were found in three additional evergreen forest ecosystems in South China (Tan et al., 2012; Yan et al., 2013; Yu et al., 2008; LM Zhang et al., 2006) and the Kiryu temperate evergreen coniferous forest in Japan (Takanashi et al., 2005). Our results (Fig. 5 and Table 3) also proved that the temperate forests (e.g., the ALS and LJ) acted as the strongest carbon sinks (Jung et al., 2017; Kondo et al., 2017; Luyssaert et al., 2007; Yu et al., 2014a). Additionally, the carbon sinks in the ALS (broad-leaved) and LJ (coniferous) were higher than those in the corresponding forest ecosystems in China (Table 3). In addition, a review of a large dataset concluded that the mean global NEE in boreal and temperate forest ecosystems was −2.2 ± 0.1 tC ha^{-1} yr^{-1} (Luyssaert et al., 2008), which means that the average NEE in the ALS and LJ (−5.54 tC ha^{-1} yr^{-1}) was exceptional on a global basis and that these ecosystems may be regarded as significant contributors to the global forest carbon sink.

Strong seasonality was observed for the carbon sink in the tropical forest (XSBN), with a modest carbon sink during the dry season (1.30 tC ha^{-1}) but a weak carbon source during the wet season (Fig. 5). Generally, this seasonality matched other results (Baldocchi et al., 2017; Hutyra et al., 2007; Saleska et al., 2003; Tan et al., 2010). Here, the reasons for the seasonality seemed to be the high temperature and soil moisture during the wet season, which resulted in a high R_{eco} (Anderegg et al., 2015; Hutyra et al., 2007; Wang

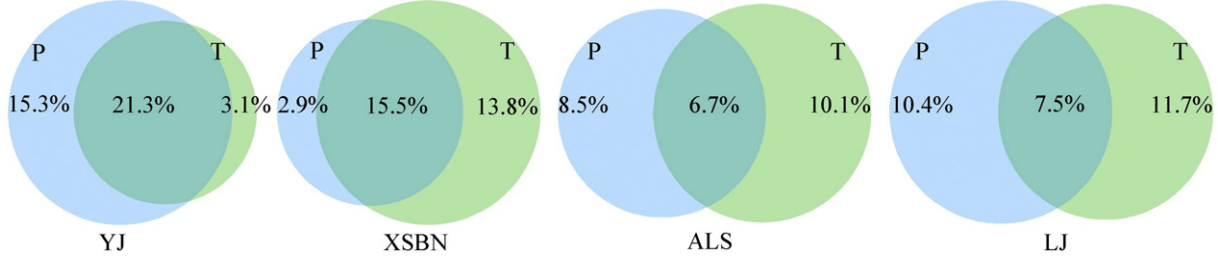

Fig. 8. Contributions from critical climatic factors (T and P) to the variations in the NEE in Yunnan's typical forest ecosystems (YJ, XSBN, ALS, and LJ) in SW China.

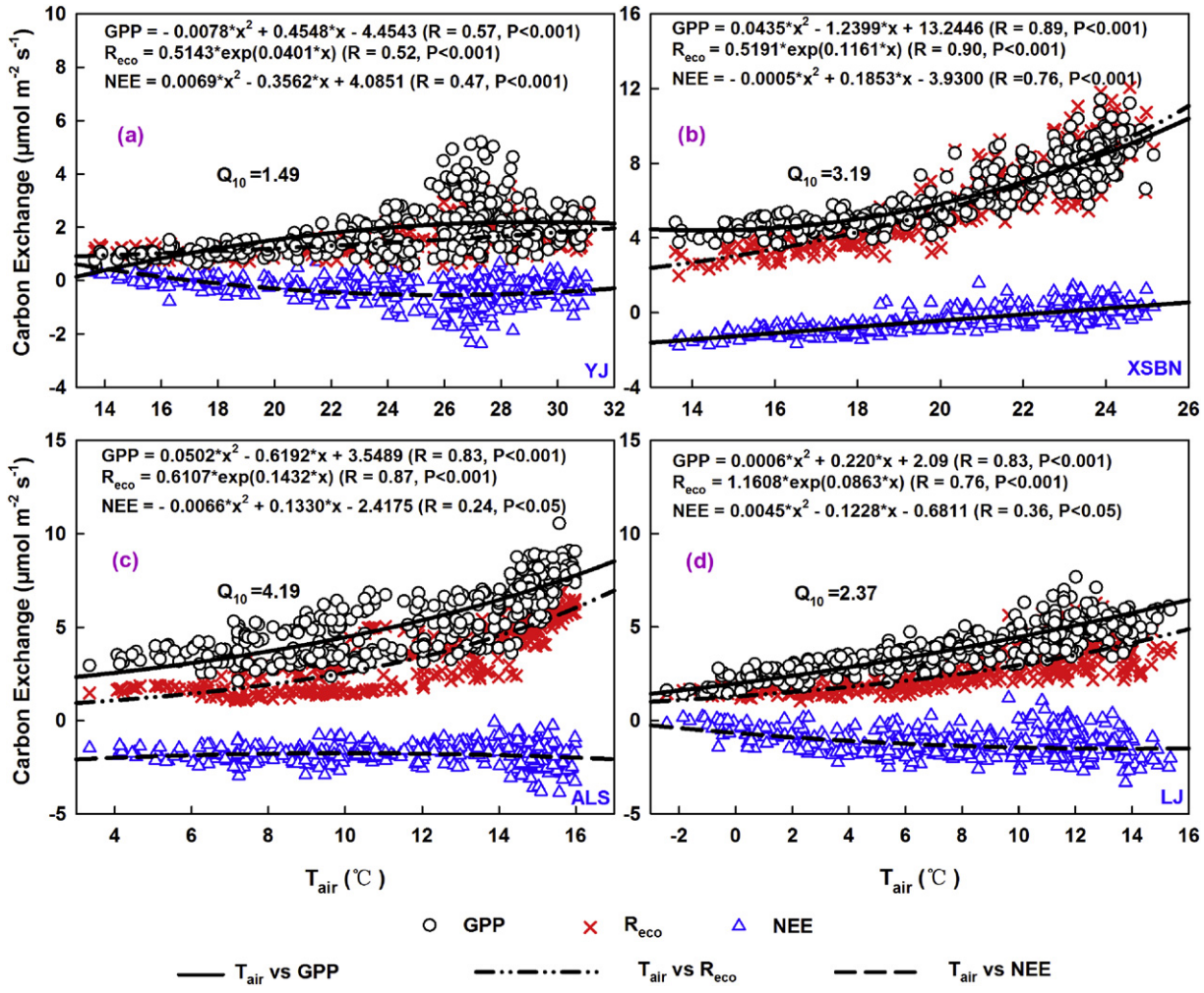

Fig. 9. Regression analysis between the carbon exchange (GPP, R_{eco}, and NEE) and air temperature (T_{air}, °C) at a daily time scale in the Yuanjiang semi-arid savanna ecosystem (a), Xishuangbanna tropical rainforest ecosystem (b), Ailaoshan subtropical evergreen broad-leaved forest ecosystem (c) and Lijiang subalpine coniferous forest ecosystem (d) in Yunnan Province, Southwest China. The Q_{10} values were calculated according to the Van't Hoff equation (Peng et al., 2009; Van't Hoff and Lehfeldt, 1899). Negative NEE values mean that the ecosystem uptakes CO_2 from the atmosphere and creates a carbon sink, while positive NEE values mean the release of CO_2 into the atmosphere. The data were multiyear daily averaged values.

et al., 2014), so the respiration exceeded the photosynthesis and triggered carbon release (Tan et al., 2010; Zhang et al., 2010). The 14-year mean annual NEE in the tropical forest was −1.25 tC ha^{-1} yr^{-1}, which was lower than the 4-year inventory-based NEP (3.59 tC ha^{-1} yr^{-1}) (Tan et al., 2010). The main reason for this result may have been a consecutive 3-year drought that occurred from 2009 to 2011, which decreased the carbon sink. In addition, the carbon sink was lower than that in a 33-year-old rubber plantation that was 10 km from the XSBN, where the eddy covariance and inventory-based NEP was 7.9 and 9.04 tC ha^{-1} yr^{-1}, respectively, due to fertilizer input and other management practices (Song et al., 2014). However, our finding was similar to the carbon sink in a tropical rainforest ecosystem in the Southwest Amazon (−1.02 tC ha^{-1} yr^{-1}) (Grace et al., 1995) and another tropical rainforest ecosystem at Pasoh in Malaysia, where the three-year average NEE was −1.24 tC ha^{-1} yr^{-1} (Kosugi et al., 2008). A study in Asian terrestrial ecosystems concluded that tropical Asia acts as a carbon sink with a mean annual NEE of −1.80 tC ha^{-1} yr^{-1} (Kato and Tang, 2008). Furthermore, many larger-scale studies have found that tropical rainforest ecosystems serve as carbon sinks (Gatti et al., 2014; Grace et al., 2014; Pan et al., 2011) and that the average GPP, R_{eco}, and NEE from some global tropical forests are 31.14, 30.11, and −0.84 tC ha^{-1} yr^{-1} (Table 3), although a few tropical rainforest ecosystems have been found to be carbon sources (Hutyra et al., 2007; Kato and Tang, 2008).

In the savanna (YJ), approximately 84% of the annual NEE (−1.29 tC ha^{-1} yr^{-1}) occurred during the wet season, while −0.21 tC ha^{-1} yr^{-1} occurred during the dry season (Fig. 5), although high MAT and VPD were found in the YJ (Fig. 3 and Table 2). This carbon-sink strength was consistent with the published inventory at the same site (0.96 tC ha^{-1} yr^{-1}) (Fei et al., 2017). Many studies found that the carbon sinks in savannas mainly occur during the wet season (Ago et al., 2014; Ardo et al., 2008; Chen et al., 2003; Grace et al., 2006; Ivans et al., 2006; Quansah et al., 2015; Santos et al., 2003; Veenendaal et al., 2004). Therefore, approximately 84% of the NEE could have occurred during the wet season in this savanna (−1.08 tC ha^{-1} yr^{-1}), while the dry season was nearly carbon neutral. A synthesis of carbon-flux data in nearly 20 global savanna ecosystems (Fei et al., 2017) showed that most savanna ecosystems act as carbon sinks and that the amplitude of the NEE ranges from approximately 1.3 to −3.9 tC ha^{-1} yr^{-1} (the average GPP, R_{eco}, and NEE were 10.13 ± 4.66, 8.78 ± 3.79 and −1.34 ± 1.58 tC ha^{-1} yr^{-1}, respectively (Table 3). This study's data are consistent with these results based on the above statements.

The reported fluxes in this work provide further confirmation that old forests (e.g., the XSBN, ALS, and LJ; see details in Table 1) are acting as carbon sinks (Lewis et al., 2009; Luyssaert et al., 2008; Zhou et al., 2006). However, the average NEE was −3.40 tC ha^{-1} yr^{-1} in Yunnan (Table 3), which was higher than the reported rates from European forest ecosystems (−1.97 tC ha^{-1} yr^{-1}) (Luyssaert et al., 2010),

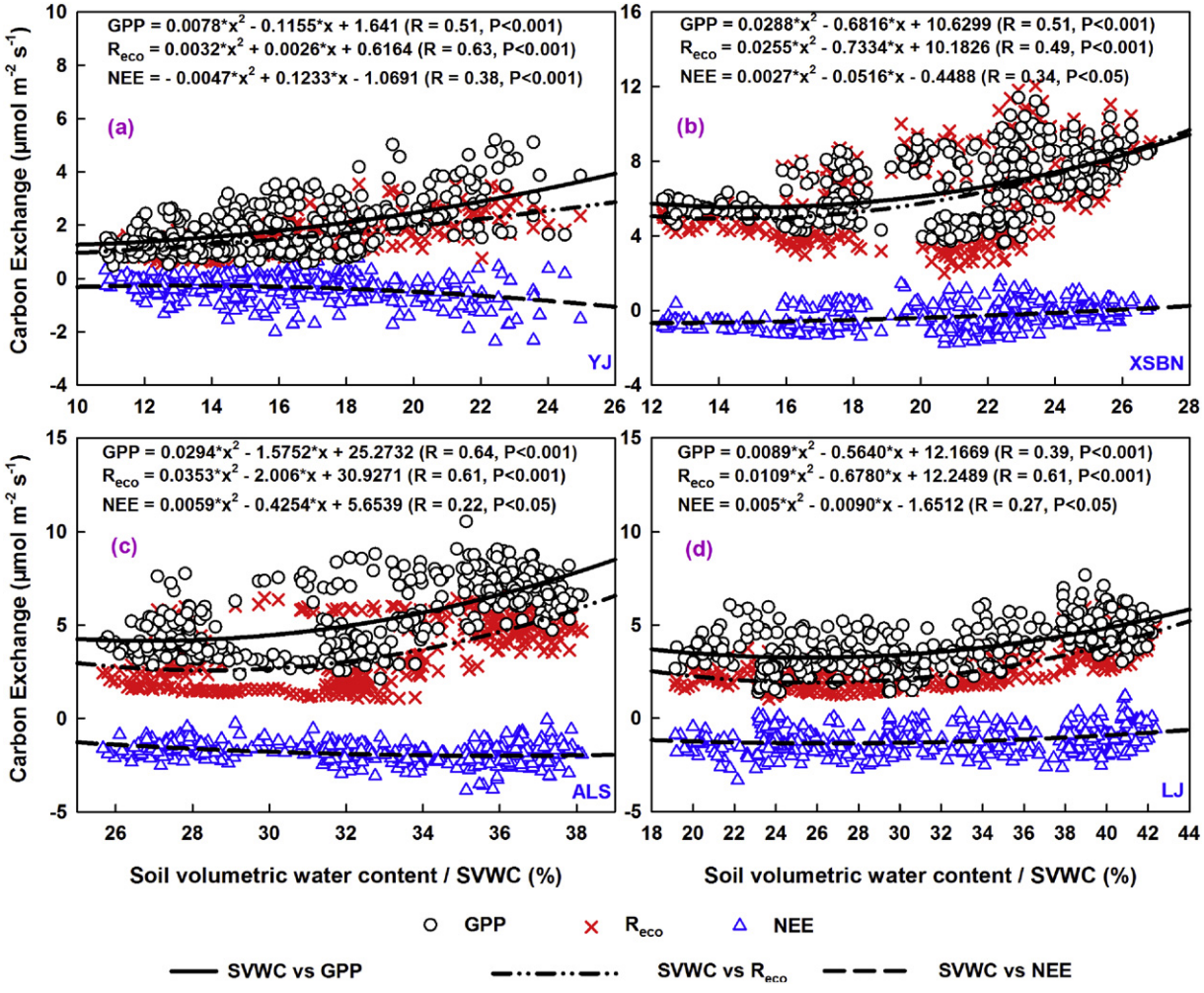

Fig. 10. Regression analysis between the carbon exchange (GPP, R_{eco}, NEE) and soil volumetric water content (SVWC, %) at a daily time scale in the Yuanjiang semi-arid savanna ecosystem (a), Xishuangbanna tropical rainforest ecosystem (b), Ailaoshan subtropical evergreen broad-leaved forest ecosystem (c) and Lijiang subalpine coniferous forest ecosystem (d) in Yunnan Province, Southwest China. The dataset were multiyear daily averaged values.

Asian/global forest ecosystems (−2.74, and −2.22 tC ha^{-1} yr^{-1}, respectively), and Asian/global terrestrial ecosystems (−2.32, and −1.34 tC ha^{-1} yr^{-1}, respectively) (Table 3). We may conclude that the old-growth forest ecosystems in Yunnan are currently playing an important role in the regional and global carbon cycle and mitigating the global increase in CO_2.

4.2. Correlations among the R_{eco} and NEP with the GPP

The correlations between the R_{eco} and NEP with the GPP provide insights into the mechanism of carbon exchange and may be useful in the construction of biophysical models. Others have demonstrated that the R_{eco} and NEP are positively linearly correlated with the GPP, especially R_{eco} with GPP (Beringer et al., 2016; Chen et al., 2015; Lasslop et al., 2010; GR Yu et al., 2013a). In this work, combining data from all four sites showed that R_{eco} was highly coupled with the GPP in a roughly linear fashion (Fig. 6), which matched other findings elsewhere (Baldocchi et al., 2017; Chen et al., 2015; Lasslop et al., 2010; Valentini et al., 2000; Yu et al., 2008; GR Yu et al., 2013a). The relationships between the GPP and NEP were less clear. We found a parabolic relationship whereby the NEP decreased when the GPP > 17.5 tC ha^{-1} yr^{-1} (Fig. 6). This pattern contrasts previous results, in which the NEP was linearly and positively correlated with the GPP (Law et al., 2002; GR Yu et al., 2013a). The trend in our study is likely more reasonable and realistic to reveal the correlation between the NEP and GPP in forest ecosystems because 1) the previous dataset included a few NEP and GPP values in tropical ecosystems (or constrained the GPP dataset to a specific range: GPP < 22.0 tC ha^{-1} yr^{-1}) (Law et al., 2002), while many subtropical, temperate, boreal forest, and many other ecosystems (cropland, grassland, and wetland) have been investigated in previous studies (Baldocchi et al., 2017; Law et al., 2002; GR Yu et al., 2013a) and the structure of the dataset remarkably affected the regression results; and 2) the latitude trend in the NEP demonstrates that the mid-latitude has a stronger carbon sink (Kato and Tang, 2008; Kondo et al., 2017; Yu et al., 2014a) and that tropical forest ecosystems (lower latitude) have a larger GPP than mid-latitude ecosystems. Thus, the ratio between the NEP and GPP in tropical forests should be lower than that in subtropical or other ecosystems. Thus, a key finding in this research was that the NEP decreased when the GPP was greater than some threshold and that their relationship is best expressed as a quadratic model.

4.3. Effects of temperature and precipitation on carbon exchange

In this study, path analysis and RDA were applied to suggest the quantitative effects of control factors (T, P, and VPD) on carbon sinks. This analysis must be regarded as tentative because of the strong inter-correlations between the environmental variables. Notwithstanding this difficulty, the NEP was controlled mainly by the VPD and P in the YJ (the PCs were −0.69 and 0.46, respectively) but by T in the XSBN, ALS and LJ. Interestingly, we found that T had a strongly negative (PC = −0.54) influence on the NEP in the XSBN but a positive influence in the ALS and LJ (Fig. 7). RDA was then applied to quantify the effects of

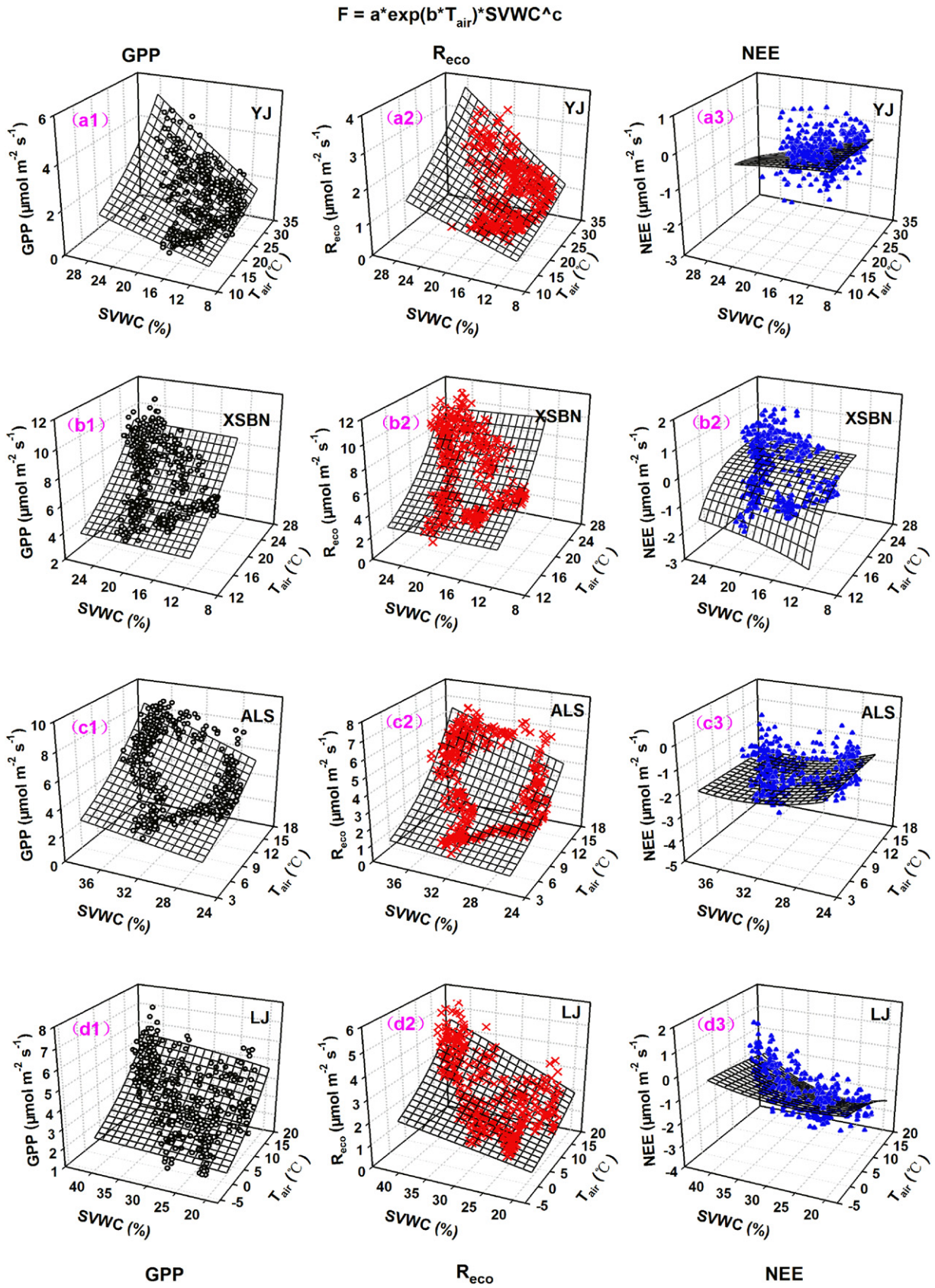

Fig. 11. Interaction of the air temperature (T_{air}, °C) and soil volumetric water content (SVWC, %) on the GPP (a1–d1), R_{eco} (a2–d2), and NEE (a3–d3) at a daily time scale in the Yuanjiang semi-arid savanna ecosystem (a), Xishuangbanna tropical rainforest ecosystem (b), Ailaoshan subtropical evergreen broad-leaved forest ecosystem (c) and Lijiang subalpine coniferous forest ecosystem (d) in Yunnan Province, Southwest China. The data were multiyear daily averaged values.

Table 3
Comparison of the carbon exchange over different biomes and regions.

Vegetation/biome		Synthesis of previous studies (tC ha^{-1} yr^{-1})				In this study (tC ha^{-1} yr^{-1})		
		GPP	R_{eco}	NEE	References	GPP	R_{eco}	NEE
Biome	Savanna	10.13	8.78	−1.34	a	6.90	5.62	−1.28
	Tropical forest	31.14	30.11	−0.84	b	25.47	24.22	−1.25
	Broad-leaved forest	15.46	11.17	−4.10	(Li, 2014)	20.68	13.66	−7.02
	Coniferous forest	13.46	10.49	−2.97	(Li, 2014)	13.92	9.87	−4.05
	Mean	17.16	14.80	−2.34		16.74	13.34	−3.40
China	Forest ecosystem			−3.50	(GR Yu et al., 2013a)			
	Terrestrial ecosystem			−2.53	(GR Yu et al., 2013a)			
Asian	Forest ecosystem	16.91	14.28	−2.74	(Chen et al., 2013)			
	Terrestrial ecosystem	11.82	9.9	−2.32	(Chen et al., 2013)			
Globally	Forest ecosystem			−2.22	c			
	Forest ecosystem			−1.23	(Pan et al., 2011)			
	Terrestrial ecosystem	9.35	8.01	−1.34	(Jung et al., 2011)			
	Terrestrial ecosystem			−1.56	d			

Note: a) Average GPP, R_{eco}, and NEE from some global savanna ecosystems; specific information is listed in the supplementary materials (Table S2); b) average carbon exchange from >50 site-years of data from global tropical forest ecosystems (Hirata et al., 2008; Hutyra et al., 2007; Kato and Tang, 2008; Kosugi et al., 2008; Loescher et al., 2003; Luyssaert et al., 2007; Malhi, 2012; Malhi et al., 2009; Saleska et al., 2003; Yamamoto et al., 2005), more details are provided in the supplementary materials (Table S3); c) values that were calculated from the global NEP (Jung et al., 2011; Yu et al., 2014a) and global forest area (FAO, 2015); d) values that were based on a comprehensive database (>1400 site-years of NEE values) (Baldocchi, 2014).

T and P on the carbon sink: T and P jointly explained 39.7%, 32.2%, 25.3%, and 29.6% of the variations in the NEE in the YJ, XSBN, ALS and LJ, respectively (Fig. 8). Based on the path analysis and RDA, we may draw the conclusion that the precipitation determines the NEP in semi-arid savanna ecosystems (e.g., the YJ) (Beringer et al., 2011; Beringer et al., 2016), whereas the temperature determines the NEP in tropical forest ecosystems (e.g., the XSBN) and the NEP is determined by both T and P in temperate ecosystems (e.g., ALS, and LJ) (Figs. 7 and 8). Overall, the temperature had a greater influence on the NEP than the precipitation (Figs. 7, 8, S4, and S5). Additionally, T and P generally play key roles in carbon exchange (Anderson-Teixeira et al., 2011; Baldocchi et al., 2017; Chen et al., 2013; Jung et al., 2017; Wu et al., 2011; Yu et al., 2010; GR Yu et al., 2013a), we thereafter used T and P as the main control factors in the regression analysis of the responses of carbon fluxes to determinants. The results are as follows.

The carbon sinks might significantly weaken in the YJ and XSBN under increasing temperature (Figs. 9 and S2). Interestingly, the carbon-uptake mechanism under warming was not the same as that under increasing temperature: the GPP decreased but R_{eco} increased in the YJ, thus decreasing the carbon sink. In contrast, both GPP and R_{eco} increased in the XSBN, but R_{eco} outpaced the GPP and thus decreased the carbon sink (Figs. 9 and S2). Studies also showed that warming decreased the NEP in savanna ecosystems (Cleverly et al., 2013; Fei et al., 2017; Kanniah et al., 2011) and increased R_{eco} significantly more than the GPP in tropical forest ecosystems, which weakened the NEP (Baldocchi et al., 2017; Wang et al., 2013; Wang et al., 2014; Zhang et al., 2010). In addition, the CV of the NEE was high (Fig. S1), and T had a negative effect on the carbon sinks in the XSBN and YJ (Fig. 7). Thus, carbon sequestration might decrease in both the YJ and XSBN under future warming.

In contrast, the carbon sink may increase in the ALS and LJ (Figs. 9, 11, and S2) because of the lower MAT and relative abundance of MAP in the ALS and LJ (Fig. 3b, e and Table 2). A study that was based on a 93-site-year database showed that warming may increase the carbon sinks in European forest ecosystems (Reichstein et al., 2007), while a meta-analysis suggested that warming may slightly increase the carbon uptake (Wu et al., 2011), and a 403-site-year database study concluded that climate warming might enhance the carbon sinks in boreal and temperate ecosystems (Grant et al., 2009; Zhang et al., 2017). Additionally, forest ecosystems in mid-latitude regions (with a generally higher MAT than high-latitude regions) had stronger carbon sequestration than high-latitude regions (Kato and Tang, 2008; Kondo et al., 2017; Yu et al., 2014a), which also demonstrated that slight warming in lower-MAT regions favors a stronger carbon sink. In addition, nitrogen deposition and increasing CO_2 concentration is expected to enhance photosynthesis and increase the carbon sink (Baldocchi et al., 2017; Campbell et al., 2017; Reay et al., 2008; Wang et al., 2017; Wenzel et al., 2016; Yu et al., 2014a).

Meanwhile, changes in precipitation and soil moisture caused significant variations in the NEE in the YJ and XSBN but had only a slight influence on the NEE in the ALS and LJ (Figs. 10 and S3). Precipitation is expected to increase in most regions in China, especially in the northwest and northeast (IPCC, 2013), but this factor may decrease in most of the southwest (e.g., Yunnan Province) (Gao et al., 2012; Wu et al., 2016). Thus, variations in P might have negligible effects on the carbon sinks in the ALS and YJ (Figs. 10 and S3) because of the moisture availability and lower temperatures (Table 2). By contrast, the carbon sink in the YJ might diminish (Figs. 10 and S3) because of the strong effect of precipitation in determining the NEE in savanna ecosystems (Archibald et al., 2009; Fei et al., 2017; Jia et al., 2014; Kanniah et al., 2011; Merbold et al., 2009). However, decreasing precipitation reduced both the GPP and R_{eco} in the XSBN (Figs. 10 and S3), which also mitigated the warming effects on R_{eco} (Wang et al., 2014) because the sensitivity of CO_2 emissions to temperature is regulated by SVWC (Wang et al., 2013). We also found that T had dominant effects on the carbon sink in the XSBN (Fig. 7), which is regulated by P (Fig. 8) even though P had a smaller effect on NEP (Fig. 7). Accordingly, the P decrease in the XSBN may enhance the carbon sink slightly (Figs. 10 and S3) and may compensate for the warming effect. Therefore, some uncertainty exists regarding future carbon-sink variations in the XSBN.

According to the above discussion, the carbon sink might decrease in the YJ (savanna ecosystem) under warming and decreased precipitation, but the effect at the XSBN (tropical forest ecosystem) is somewhat uncertain. In contrast, the carbon sinks may increase in the ALS and LJ (temperate forest ecosystems). However, these contrasting changes in the carbon sinks may depend on the magnitudes of the variations in T and P alongside the seasonality and other factors.

Acknowledgments

We would like to thank the editorial members of the journal and the two reviewers (Hank Loescher and another anonymous reviewer) for their constructive comments and suggestions and the staff and technicians of the Yuanjiang Research Station for Savanna Ecosystems, the Xishuangbanna Station for Tropical Rainforest Ecosystem Studies, the Ailaoshan Station for Subtropical Forest Ecosystem Studies, the Public Technology Service Center of Xishuangbanna Tropical Botanical Garden, Chinese Academy of Sciences, and the Lijiang Forest Ecosystem Research Station of Kunming Institute of Botany, Chinese Academy of Sciences for their invaluable contributions to the instruments'

maintenance, fieldwork and data collection. And this study was supported by the Joint Foundation from the National Natural Science Foundation of China and the Natural Science of the Yunnan Province (U1602234 and U1202234), the National Natural Science Foundation of China1 (NSFC) (41671209, 41405143, and 31290221), the National Key Research and Development Program of China (2016YFC0502105), CAS-JSPS Cooperative Research Project (GJHZ1521), and the Strategic Priority Research Program of the Chinese Academy of Sciences (XDA05050601 and XDA05050206), Chinese Academy of Sciences President's International Fellowship Initiative (2017VCA0036).

Competing financial interests

The authors declare no competing financial interests.

Appendix A. Supplementary data

Supplementary data to this article can be found online at https://doi.org/10.1016/j.scitotenv.2017.10.239.

References

Ago, E.E., Agbossou, E.K., Galle, S., Cohard, J.M., Heinesch, B., Aubinet, M., 2014. Long term observations of carbon dioxide exchange over cultivated savanna under a Sudanian climate in Benin (West Africa). Agric. For. Meteorol. 197, 13–25.
Anderegg, W.R., Ballantyne, A.P., Smith, W.K., Majkut, J., Rabin, S., Beaulieu, C., et al., 2015. Tropical nighttime warming as a dominant driver of variability in the terrestrial carbon sink. Proc. Natl. Acad. Sci. U. S. A. 112, 15591–15596.
Anderson, K., Peters, G., 2016. The trouble with negative emissions. Science 354, 182–183.
Anderson-Teixeira, K.J., Delong, J.P., Fox, A.M., Brese, D.A., Litvak, M.E., 2011. Differential responses of production and respiration to temperature and moisture drive the carbon balance across a climatic gradient in New Mexico. Glob. Chang. Biol. 17, 410–424.
Archibald, S.A., Kirton, A., van der Merwe, M.R., Scholes, R.J., Williams, C.A., Hanan, N., 2009. Drivers of inter-annual variability in Net Ecosystem Exchange in a semi-arid savanna ecosystem, South Africa. Biogeosciences 6, 251–266.
Ardo, J., Molder, M., El-Tahir, B.A., Elkhidir, H.A., 2008. Seasonal variation of carbon fluxes in a sparse savanna in semi-arid Sudan. Carbon Balance Manag. 3, 7.
Aubinet, M., Chermanne, B., Vandenhaute, M., Longdoz, B., Yernaux, M., Laitat, E., 2001. Long term carbon dioxide exchange above a mixed forest in the Belgian Ardennes. Agric. For. Meteorol. 108, 293–315.
Baldocchi, D., 2003. Assessing the eddy covariance technique for evaluating carbon dioxide exchange rates of ecosystems: past, present and future. Glob. Chang. Biol. 9, 479–492.
Baldocchi, D., 2008. 'Breathing' of the terrestrial biosphere: lessons learned from a global network of carbon dioxide flux measurement systems. Aust. J. Bot. 56, 1–26.
Baldocchi, D., 2014. Measuring fluxes of trace gases and energy between ecosystems and the atmosphere - the state and future of the eddy covariance method. Glob. Chang. Biol. 20, 3600–3609.
Baldocchi, D., Valentini, R., Running, S., Oechel, W., Dahlman, R., 1996. Strategies for measuring and modelling carbon dioxide and water vapour fluxes over terrestrial ecosystems. Glob. Chang. Biol. 2, 159–168.
Baldocchi, D., Finnigan, J., Wilson, K., Paw, U.K.T., Falge, E., 2000. On measuring net ecosystem carbon exchange over tall vegetation on complex terrain. Bound.-Layer Meteorol. 96, 257–291.
Baldocchi, D., Falge, E., Gu, L.H., Olson, R., Hollinger, D., Running, S., et al., 2001a. FLUXNET: a new tool to study the temporal and spatial variability of ecosystem-scale carbon dioxide, water vapor, and energy flux densities. Bull. Am. Meteorol. Soc. 82, 2415–2434.
Baldocchi, D., Falge, E., Wilson, K., 2001b. A spectral analysis of biosphere-atmosphere trace gas flux densities and meteorological variables across hour to multi-year time scales. Agric. For. Meteorol. 107, 1–27.
Baldocchi, D., Chu, H., Reichstein, M., 2017. Inter-annual variability of net and gross ecosystem carbon fluxes: a review. Agric. For. Meteorol. https://doi.org/10.1016/j.agrformet.2017.05.015.
Bassow, S.L., Bazzaz, F.A., 1998. How environmental conditions affect canopy leaf-level photosynthesis in four deciduous tree species. Ecology 79, 2660–2675.
Beringer, J., Hutley, L.B., Hacker, J.M., Neininger, B., Paw, U.K.T., 2011. Patterns and processes of carbon, water and energy cycles across northern Australian landscapes: from point to region. Agric. For. Meteorol. 151, 1409–1416.
Beringer, J., Hutley, L.B., McHugh, I., Arndt, S.K., Campbell, D., Cleugh, H.A., et al., 2016. An introduction to the Australian and New Zealand flux tower network-OzFlux. Biogeosci. Discuss. 13, 1–52.
Bracho, R., Starr, G., Gholz, H.L., Martin, T.A., Cropper, W.P., Loescher, H.W., 2012. Controls on carbon dynamics by ecosystem structure and climate for southeastern U.S. slash pine plantations. Ecol. Monogr. 82, 101–128.
Campbell, J.E., Berry, J.A., Seibt, U., Smith, S.J., Montzka, S.A., Launois, T., et al., 2017. Large historical growth in global terrestrial gross primary production. Nature 544, 84–87.
Cao, M., Zou, X., Warren, M., Zhu, H., 2006. Tropical forests of Xishuangbanna, China. Biotropica 38, 306–309.
Carrara, A., Kowalski, A.S., Neirynck, J., Janssens, I.A., Yuste, J.C., Ceulemans, R., 2003. Net ecosystem CO_2 exchange of mixed forest in Belgium over 5 years. Agric. For. Meteorol. 119, 209–227.
Chan, O.C., Yang, X., Fu, Y., Feng, Z., Sha, L., Casper, P., et al., 2006. 16S rRNA gene analyses of bacterial community structures in the soils of evergreen broad-leaved forests in south-west China. FEMS Microbiol. Ecol. 58, 247–259.
Chapin, F.S., Woodwell, G.M., Randerson, J.T., Rastetter, E.B., Lovett, G.M., Baldocchi, D.D., et al., 2006. Reconciling carbon-cycle concepts, terminology, and methods. Ecosystems 9, 1041–1050.
Chapin, F.S., Matson, P.A., Vitousek, P.M., 2011. Principles of Terrestrial Ecosystem Ecology. Springer, New York, USA.
Chen, X., Hutley, L.B., Eamus, D., 2003. Carbon balance of a tropical savanna of northern Australia. Oecologia 137, 405–416.
Chen, Z., GR, Yu, Ge, J.P., Sun, X.M., Hirano, T., Saigusa, N., et al., 2013. Temperature and precipitation control of the spatial variation of terrestrial ecosystem carbon exchange in the Asian region. Agric. For. Meteorol. 182, 266–276.
Chen, Z., Yu, G., Zhu, X., Wang, Q., Niu, S., Hu, Z., 2015. Covariation between gross primary production and ecosystem respiration across space and the underlying mechanisms: a global synthesis. Agric. For. Meteorol. 203, 180–190.
Ciais, P., Reichstein, M., Viovy, N., Granier, A., Ogee, J., Allard, V., et al., 2005. Europe-wide reduction in primary productivity caused by the heat and drought in 2003. Nature 437, 529–533.
Cleverly, J., Boulain, N., Villalobos-Vega, R., Grant, N., Faux, R., Wood, C., et al., 2013. Dynamics of component carbon fluxes in a semi-arid Acacia woodland, central Australia. J. Geophys. Res.-Biogeosci. 118, 1168–1185.
De'ath, G., Fabricius, K.E., 2000. Classification and regression trees: a powerful yet simple technique for ecological data analysis. Ecology 81, 3178–3192.
Falge, E., Baldocchi, D., Olson, R., Anthoni, P., Aubinet, M., Bernhofer, C., et al., 2001. Gap filling strategies for defensible annual sums of net ecosystem exchange. Agric. For. Meteorol. 107, 43–69.
Falge, E., Baldocchi, D., Tenhunen, J., Aubinet, M., Bakwin, P., Berbigier, P., et al., 2002. Seasonality of ecosystem respiration and gross primary production as derived from FLUXNET measurements. Agric. For. Meteorol. 113, 53–74.
Fang, J.Y., Chen, A.P., Peng, C.H., Zhao, S.Q., Ci, L.J., 2001. Changes in forest biomass carbon storage in China between 1949 and 1998. Science 292, 2320–2322.
FAO, 2015. Global Forest Resources Assessment 2015: How Are the World's Forests Changing. Food and Agriculture Organization of the United Nations (FAO), Rome.
Fei, X.H., ZHang, Y.P., Song, Q.H., Li, P.G., Liu, Y.T., Jin, Y.Q., et al., 2016. Characteristics of solar radiation distribution and albedo in Yuanjiang dry-hot valley, Southwest China. J. Beijing For. Univ. 38, 1–10.
Fei, X.H., Jin, Y.Q., Zhang, Y.P., Sha, L.Q., Liu, Y.T., Song, Q.H., et al., 2017. Eddy covariance and biometric measurements show that a savanna ecosystem in Southwest China is a carbon sink. Sci Rep 7. https://doi.org/10.1038/srep41025.
Fox, J., Nie, Z., Byrnes, J., Culbertson, M., DebRoy, S., Friendly, M., et al., 2016. sem: Structural Equation Models. R package version 3.1-8. https://CRAN.R-project.org/package=sem.
Frank, D., Reichstein, M., Bahn, M., Thonicke, K., Frank, D., Mahecha, M.D., et al., 2015. Effects of climate extremes on the terrestrial carbon cycle: concepts, processes and potential future impacts. Glob. Chang. Biol. 21, 2861–2880.
Gao, X.J., Shi, Y., Zhang, D.F., Giorgi, F., 2012. Climate change in China in the 21st century as simulated by a high resolution regional climate model. Chin. Sci. Bull. 57, 1188–1195.
Gatti, L.V., Gloor, M., Miller, J.B., Doughty, C.E., Malhi, Y., Domingues, L.G., et al., 2014. Drought sensitivity of Amazonian carbon balance revealed by atmospheric measurements. Nature 506, 76–80.
Gilmanov, T.G., Soussana, J.E., Aires, L., Allard, V., Ammann, C., Balzarolo, M., et al., 2007. Partitioning European grassland net ecosystem CO_2 exchange into gross primary productivity and ecosystem respiration using light response function analysis. Agric. Ecosyst. Environ. 121, 93–120.
Goulden, M.L., Munger, J.W., Fan, S.M., Daube, B.C., Wofsy, S.C., 1996. Measurements of carbon sequestration by long-term eddy covariance: methods and a critical evaluation of accuracy. Glob. Chang. Biol. 2, 169–182.
Grace, J.B., Bollen, K.A., 2005. Interpreting the results from multiple regression and structural equation models. America]–>Bull. Ecol. Soc. Am. 86, 283–295.
Grace, J., Lloyd, J., McIntyre, J., Miranda, A.C., 1995. Carbon dioxide uptake by an undisturbed tropical rain forest in southwest Amazonia, 1992 to 1993. Science 270, 778.
Grace, J., San Jose, J., Meir, P., Miranda, H.S., Montes, R.A., 2006. Productivity and carbon fluxes of tropical savannas. J. Biogeogr. 33, 387–400.
Grace, J., Mitchard, E., Gloor, E., 2014. Perturbations in the carbon budget of the tropics. Glob. Chang. Biol. 20, 3238–3255.
Grant, R.F., Margolis, H.A., Barr, A.G., Black, T.A., Dunn, A.L., Bernier, P.Y., et al., 2009. Changes in net ecosystem productivity of boreal black spruce stands in response to changes in temperature at diurnal and seasonal time scales. Tree Physiol. 29, 1–17.
Heimann, M., Reichstein, M., 2008. Terrestrial ecosystem carbon dynamics and climate feedbacks. Nature 451, 289–292.
Hirata, R., Saigusa, N., Yamamoto, S., Ohtani, Y., Ide, R., Asanuma, J., et al., 2008. Spatial distribution of carbon balance in forest ecosystems across East Asia. Agric. For. Meteorol. 148, 761–775.
Hollinger, D.Y., Kelliher, F.M., Byers, J.N., Hunt, J.E., Mcseveny, T.M., Weir, P.L., 1994. Carbon-dioxide exchange between an undisturbed old-growth temperate forest and the atmosphere. Ecology 75, 134–150.
Huang, H., Chen, Z.F., Liu, D.T., He, G.X., He, R.H., Li, D.Z., et al., 2017. Species composition and community structure of the Yulongxueshan (Jade Dragon Snow Mountains) forest dynamics plot in the cold temperate spruce-fir forest, Southwest China. Biodivers. Sci. 25, 255–264.
Hutyra, L.R., Munger, J.W., Saleska, S.R., Gottlieb, E., Daube, B.C., Dunn, A.L., et al., 2007. Seasonal controls on the exchange of carbon and water in an Amazonian rain forest. J. Geophys. Res.: Biogeosci. (2005–2012) 112.

Huxman, T.E., Turnipseed, A.A., Sparks, J.P., Harley, P.C., Monson, R.K., 2003. Temperature as a control over ecosystem CO_2 fluxes in a high-elevation, subalpine forest. Oecologia 134, 537–546.
IPCC, 2013. Climate change 2013: the physical science basis. Contribution of Working Group I to the Fifth Assessment Report of the Intergovernmental Panel on Climate Change. Cambridge University Press, Cambridge, United Kingdom and New York, NY, USA.
Ivans, S., Hipps, L., Leffler, A.J., Ivans, C.Y., 2006. Response of water vapor and CO_2 fluxes in semiarid lands to seasonal and intermittent precipitation pulses. J. Hydrometeorol. 7, 995–1010.
Jia, X., Zha, T.S., Wu, B., Zhang, Y.Q., Gong, J.N., Qin, S.G., et al., 2014. Biophysical controls on net ecosystem CO2 exchange over a semiarid shrubland in northwest China. Biogeosciences 11, 4679–4693.
Jia, X., Zha, T., Gong, J., Wang, B., Zhang, Y., Wu, B., et al., 2016. Carbon and water exchange over a temperate semi-arid shrubland during three years of contrasting precipitation and soil moisture patterns. Agric. For. Meteorol. 228–229, 120–129.
Jung, M., Reichstein, M., Margolis, H.A., Cescatti, A., Richardson, A.D., Arain, M.A., et al., 2011. Global patterns of land-atmosphere fluxes of carbon dioxide, latent heat, and sensible heat derived from eddy covariance, satellite, and meteorological observations. J. Geophys. Res.-Biogeosci. 116.
Jung, M., Reichstein, M., Schwalm, C.R., Huntingford, C., Sitch, S., Ahlstrom, A., et al., 2017. Compensatory water effects link yearly global land CO_2 sink changes to temperature. Nature 541, 516–520.
Kanniah, K.D., Beringer, J., Hutley, L.B., 2011. Environmental controls on the spatial variability of savanna productivity in the Northern Territory, Australia. Agric. For. Meteorol. 151, 1429–1439.
Kato, T., Tang, Y., 2008. Spatial variability and major controlling factors of CO_2 sink strength in Asian terrestrial ecosystems: evidence from eddy covariance data. Glob. Chang. Biol. 14, 2333–2348.
Knapp, A.K., Fay, P.A., Blair, J.M., Collins, S.L., Smith, M.D., Carlisle, J.D., et al., 2002. Rainfall variability, carbon cycling, and plant species diversity in a mesic grassland. Science 298, 2202–2205.
Kondo, M., Saitoh, T.M., Sato, H., Ichii, K., 2017. Comprehensive synthesis of spatial variability in carbon flux across monsoon Asian forests. Agric. For. Meteorol. 232, 623–634.
Kosugi, Y., Takanashi, S., Ohkubo, S., Matsuo, N., Tani, M., Mitani, T., et al., 2008. CO_2 exchange of a tropical rainforest at Pasoh in Peninsular Malaysia. Agric. For. Meteorol. 148, 439–452.
Lasslop, G., Reichstein, M., Papale, D., Richardson, A.D., Arneth, A., Barr, A., et al., 2010. Separation of net ecosystem exchange into assimilation and respiration using a light response curve approach: critical issues and global evaluation. Glob. Chang. Biol. 16, 187–208.
Law, B.E., Falge, E., Gu, L., Baldocchi, D.D., Bakwin, P., Berbigier, P., et al., 2002. Environmental controls over carbon dioxide and water vapor exchange of terrestrial vegetation. Agric. For. Meteorol. 113, 97–120.
Le Quéré, C., Andrew, R.M., Canadell, J.G., Sitch, S., Korsbakken, J.I., Peters, G.P., et al., 2016. Global Carbon Budget 2016. Earth System Science Data Discussions pp. 1–3.
Lee, X., Massman, W.J.A., 2010. Perspective on thirty years of the Webb, Pearman and Leuning density corrections. Bound.-Layer Meteorol. 139, 37–59.
Lee, X., Massman, W., Law, B., 2006. Handbook of Micrometeorology-A Guide for Surface Flux Measurement and Analysis. 29. Springer Science Business Media, New York.
Lewis, S.L., Lopez-Gonzalez, G., Sonké, B., Affum-Baffoe, K., Baker, T.R., Ojo, L.O., et al., 2009. Increasing carbon storage in intact African tropical forests. Nature 457, 1003–1006.
Li, C.C., 1975. Path Analysis-A Primer. 8. The Boxwood Press.
Li, X., 2014. Temporal and Spatial Distribution of Typical Terrestrial Ecosystem Carbon Budget and Its Affecting Factors in China. Institute of Geographic Sciences and Natural Resources Research. Ph.D. University of Chinese Academy of Sciences, Beijing.
Liu, W., Fox, J.E., Xu, Z., 2002. Biomass and nutrient accumulation in montane evergreen broad-leaved forest (*Lithocarpus xylocarpus* type) in Ailao Mountains, SW China. For. Ecol. Manag. 158, 223–235.
Liu, F.Y., Zhu, H., Shi, J.P., Chen, X.M., 2007. Characteristics of plant communities and their soil fertilities in dry-hot valley of Yuanjiang County, Yunnan, China. Chin. J. Appl. Environ. Biol. 13, 782–787.
Lloyd, J., Taylor, J.A., 1994. On the temperature dependence of soil respiration. Funct. Ecol. 8, 315–323.
Loescher, H.W., Oberbauer, S.F., Gholz, H., Clark, D.B., 2003. Environmental controls on net ecosystem-level carbon exchange and productivity in a Central American tropical wet forest. Glob. Chang. Biol. 9, 396–412.
Luyssaert, S., Inglima, I., Jung, M., Richardson, A., Reichstein, M., Papale, D., et al., 2007. CO_2 balance of boreal, temperate, and tropical forests derived from a global database. Glob. Chang. Biol. 13, 2509–2537.
Luyssaert, S., Schulze, E.D., Borner, A., Knohl, A., Hessenmoller, D., Law, B.E., et al., 2008. Old-growth forests as global carbon sinks. Nature 455, 213–215.
Luyssaert, S., Ciais, P., Piao, S.L., Schulze, E.D., Jung, M., Zaehle, S., et al., 2010. The European carbon balance. Part 3: forests. Glob. Chang. Biol. 16, 1429–1450.
Malhi, Y., 2012. The productivity, metabolism and carbon cycle of tropical forest vegetation. J. Ecol. 100, 65–75.
Malhi, Y., AragÃO, L.E.O.C., Metcalfe, D.B., Paiva, R., Quesada, C.A., Almeida, S., et al., 2009. Comprehensive assessment of carbon productivity, allocation and storage in three Amazonian forests. Glob. Chang. Biol. 15, 1255–1274.
Mekonnen, Z.A., Grant, R.F., Schwalm, C., 2016. Contrasting changes in gross primary productivity of different regions of North America as affected by warming in recent decades. Agric. For. Meteorol. 218–219, 50–64.
Merbold, L., Ardo, J., Arneth, A., Scholes, R.J., Nouvellon, Y., de Grandcourt, A., et al., 2009. Precipitation as driver of carbon fluxes in 11 African ecosystems. Biogeosciences 6, 1027–1041.
Nizami, S.M., Yiping, Z., Zheng, Z., Zhiyun, L., Guoping, Y., Liqing, S., 2017. Evaluation of forest structure, biomass and carbon sequestration in subtropical pristine forests of SW China. Environ. Sci. Pollut. Res. 24, 8137–8146.
Oksanen, J., 2015. Multivariate Analysis of Ecological Communities in R: Vegan Tutorial. R Package Version. 1 pp. 11–12.
Olivas, P.C., Oberbauer, S.F., Tweedie, C.E., Oechel, W.C., Kuchy, A., 2010. Responses of CO_2 flux components of Alaskan Coastal Plain tundra to shifts in water table. J. Geophys. Res. 115.
Pan, Y., Birdsey, R.A., Fang, J., Houghton, R., Kauppi, P.E., Kurz, W.A., et al., 2011. A large and persistent carbon sink in the world's forests. Science 333, 988–993.
Papale, D., Reichstein, M., Aubinet, M., Canfora, E., Bernhofer, C., Kutsch, W., et al., 2006. Towards a standardized processing of Net Ecosystem Exchange measured with eddy covariance technique: algorithms and uncertainty estimation. Biogeosciences 3, 571–583.
Peng, S., Piao, S., Wang, T., Sun, J., Shen, Z., 2009. Temperature sensitivity of soil respiration in different ecosystems in China. Soil Biol. Biochem. 41, 1008–1014.
Piao, S., Fang, J., Ciais, P., Peylin, P., Huang, Y., Sitch, S., et al., 2009. The carbon balance of terrestrial ecosystems in China. Nature 458, 1009–1013.
Qiao, N., Schaefer, D., Blagodatskaya, E., Zou, X., Xu, X., Kuzyakov, Y., 2013. Labile carbon retention compensates for CO released by priming in forest soils. Glob. Chang. Biol. 20, 1943–1954.
Qin, D.H., Ding, Y.H., Su, J.L., Ren, J., Wen, Wang, S.W., Wu, R., Sheng, et al., 2005. Assessment of climate and environment changes in China (I): climate and environment changes in China and their projection. Adv. Clim. Chang. Res. 2, 1–05.
Qing, L., 2004. Effects of gap size and with-in gap position on the survival and growth of naturally regenerated *Picea likiangensis* seedlings. Chin. J. Appl. Environ. Biol. 10, 281–285.
Quansah, E., Mauder, M., Balogun, A.A., Amekudzi, L.K., Hingerl, L., Bliefernicht, J., et al., 2015. Carbon dioxide fluxes from contrasting ecosystems in the Sudanian Savanna in West Africa. Carbon Balance Manag. 10, 1.
Randerson, J.T., Chapin, F.S., Harden, J.W., Neff, J.C., Harmon, M.E., 2002. Net ecosystem production: a comprehensive measure of net carbon accumulation by ecosystems. Ecol. Appl. 12, 937–947.
Reay, D.S., Dentener, F., Smith, P., Grace, J., Feely, R.A., 2008. Global nitrogen deposition and carbon sinks. Nat. Geosci. 1, 430–437.
Reichstein, M., Tenhunen, J.D., Roupsard, O., Ourcival, J.M., Rambal, S., Dore, S., et al., 2002. Ecosystem respiration in two Mediterranean evergreen Holm Oak forests: drought effects and decomposition dynamics. Funct. Ecol. 16, 27–39.
Reichstein, M., Falge, E., Baldocchi, D., Papale, D., Aubinet, M., Berbigier, P., et al., 2005. On the separation of net ecosystem exchange into assimilation and ecosystem respiration: review and improved algorithm. Glob. Chang. Biol. 11, 1424–1439.
Reichstein, M., Papale, D., Valentini, R., Aubinet, M., Bernhofer, C., Knohl, A., et al., 2007. Determinants of terrestrial ecosystem carbon balance inferred from European eddy covariance flux sites. Geophys. Res. Lett. 34, L01402. https://doi.org/10.1029/2006GL027880.
Reichstein, M., Bahn, M., Ciais, P., Frank, D., Mahecha, M.D., Seneviratne, S.I., et al., 2013. Climate extremes and the carbon cycle. Nature 500, 287–295.
Saito, M., Kato, T., Tang, Y., 2009. Temperature controls ecosystem CO_2 exchange of an alpine meadow on the northeastern Tibetan Plateau. Glob. Chang. Biol. 15, 221–228.
Saleska, S.R., Miller, S.D., Matross, D.M., Goulden, M.L., Wofsy, S.C., da Rocha, H.R., et al., 2003. Carbon in Amazon forests: unexpected seasonal fluxes and disturbance-induced losses. Science 302, 1554–1557.
Santos, A.J.B., Silva, G.T.D.A., Miranda, H.S., Miranda, A.C., Lloyd, J., 2003. Effects of fire on surface carbon, energy and water vapour fluxes over campo sujo savanna in central Brazil. Funct. Ecol. 17, 711–719.
Schemske, D.W., Horvitz, C.C., 1988. Plant-animal interactions and fruit production in a neotropical herb: a path analysis. Ecology 69, 1128–1137.
Song, Q.H., Tan, Z.H., Zhang, Y.P., Sha, L.Q., Deng, X.B., Deng, Y., et al., 2014. Do the rubber plantations in tropical China act as large carbon sinks? iFor.-Biogeosci. For. 7, 42–47.
Song, Q.-H., Fei, X.-H., Zhang, Y.-P., Sha, L.-Q., Liu, Y.-T., Zhou, W.-J., et al., 2017. Water use efficiency in a primary subtropical evergreen forest in Southwest China. Sci Rep 7. https://doi.org/10.1038/srep43031.
Tagesson, T., Fensholt, R., Cappelaere, B., Mougin, E., Horion, S., Kergoat, L., et al., 2016. Spatiotemporal variability in carbon exchange fluxes across the Sahel. Agric. For. Meteorol. 226–227, 108–118.
Takanashi, S., Kosugi, Y., Tanaka, Y., Yano, M., Katayama, T., Tanaka, H., et al., 2005. CO_2 exchange in a temperate Japanese cypress forest compared with that in a cool-temperate deciduous broad-leaved forest. Ecol. Res. 20, 313–324.
Tan, Z.H., Zhang, Y.P., GR, Yu, Sha, L.Q., Tang, J.W., Deng, X.B., et al., 2010. Carbon balance of a primary tropical seasonal rain forest. J. Geophys. Res.-Atmos. 115.
Tan, Z.H., Zhang, Y.P., Schaefer, D., GR, Yu, Liang, N.S., Song, Q.H., 2011. An old-growth subtropical Asian evergreen forest as a large carbon sink. Atmos. Environ. 45, 1548–1554.
Tan, Z.H., Zhang, Y.P., Liang, N.S., Hsia, Y.J., Zhang, Y.J., Zhou, G.Y., et al., 2012. An observational study of the carbon-sink strength of East Asian subtropical evergreen forests. Environ. Res. Lett. 7, 044017.
Tanner, C.B., Thurtell, G.W., 1969. Anemoclinometer Measurements of Reynolds Stress and Heat Transport in the Atmospheric Surface Layer. 82. University of Wisconsin, Madison, Wisconsin.
Ueyama, M., Iwata, H., Harazono, Y., 2014. Autumn warming reduces the CO_2 sink of a black spruce forest in interior Alaska based on a nine-year eddy covariance measurement. Glob. Chang. Biol. 20, 1161–1173.
UNFCCC, 2015. Adoption of the Paris Agreement, FCCC/CP/2015/L.9/Rev.1 United Nations New York, NY. p. 32.
Valentini, R., Matteucci, G., Dolman, A., Schulze, E.-D., Rebmann, C., Moors, E., et al., 2000. Respiration as the main determinant of carbon balance in European forests. Nature 404, 861–865.

Van't Hoff, J.H., Lehfeldt, R.A., 1899. Lectures on Theoretical and Physical Chemistry. Part 1: Chemical Dynamics. Edward Arnold, London.
Veenendaal, E.M., Kolle, O., Lloyd, J., 2004. Seasonal variation in energy fluxes and carbon dioxide exchange for a broad-leaved semi-arid savanna (Mopane woodland) in Southern Africa. Glob. Chang. Biol. 10, 318–328.
Wang, W., Ciais, P., Nemani, R.R., Canadell, J.G., Piao, S., Sitch, S., et al., 2013. Variations in atmospheric CO_2 growth rates coupled with tropical temperature. U S A]–>Proc. Natl. Acad. Sci. U. S. A. 110, 13061–13066.
Wang, X.H., Piao, S.L., Ciais, P., Friedlingstein, P., Myneni, R.B., Cox, P., et al., 2014. A two-fold increase of carbon cycle sensitivity to tropical temperature variations. Nature 506, 212–215.
Wang, R., Goll, D., Balkanski, Y., Hauglustaine, D., Boucher, O., Ciais, P., et al., 2017. Global forest carbon uptake due to nitrogen and phosphorus deposition from 1850 to 2100. Glob. Chang. Biol. 23, 4854–4872.
Webb, E.K., Pearman, G.I., Leuning, R., 1980. Correction of flux measurements for density effects due to heat and water-vapor transfer. Q. J. R. Meteorol. Soc. 106, 85–100.
Weltzin, J.F., Loik, M.E., Schwinning, S., Williams, D.G., Fay, P.A., Haddad, B.M., et al., 2003. Assessing the response of terrestrial ecosystems to potential changes in precipitation. Bioscience 53, 941–952.
Wen, X.F., Wang, H.M., Wang, J.L., GR, Yu, Sun, X.M., 2010. Ecosystem carbon exchanges of a subtropical evergreen coniferous plantation subjected to seasonal drought, 2003–2007. Biogeosciences 7, 357–369.
Wenzel, S., Cox, P.M., Eyring, V., Friedlingstein, P., 2016. Projected land photosynthesis constrained by changes in the seasonal cycle of atmospheric CO_2. Nature 538, 499–501.
Wilczak, J.M., Oncley, S.P., Stage, S.A., 2001. Sonic anemometer tilt correction algorithms. Bound.-Layer Meteorol. 99, 127–150.
Wootton, J.T., 1994. Predicting direct and indirect effects: an integrated approach using experiments and path analysis. Ecology 75, 151–165.
Wright, S., 1921. Correlation and causation. J. Agric. Res. 20, 557–585.
Wu, Z.T., Dijkstra, P., Koch, G.W., Penuelas, J., Hungate, B.A., 2011. Responses of terrestrial ecosystems to temperature and precipitation change: a meta-analysis of experimental manipulation. Glob. Chang. Biol. 17, 927–942.
Wu, S., Luo, Y., Wang, H., Gao, J.B., Li, C., 2016. Climate change impacts and adaptation in China: current situation and future prospect. Chin. Sci. Bull. 61, 1042–1054.
Wu, J., Guan, K., Hayek, M., Restrepo-Coupe, N., Wiedemann, K.T., Xu, X., et al., 2017. Partitioning controls on Amazon forest photosynthesis between environmental and biotic factors at hourly to interannual timescales. Glob. Chang. Biol. 23, 1240–1257.
Yamamoto, S., Saigusa, N., Gamo, M., Fujinuma, Y., Inoue, G., Hirano, T., 2005. Findings through the AsiaFlux network and a view toward the future. J. Geogr. Sci. 15, 142–148.
Yan, J., Zhang, Y., Yu, G., Zhou, G., Zhang, L., Li, K., et al., 2013. Seasonal and inter-annual variations in net ecosystem exchange of two old-growth forests in southern China. Agric. For. Meteorol. 182-183, 257–265.
Yu, G.R., Wen, X.F., Li, Q.K., Ming, Z.L., Ren, C.Y., Liu, Y.F., et al., 2004. Seasonal patterns and environmental response of ecosystem respiration in typical subtropical and temperate forest ecosystems in China. Sci. China Ser. D: Earth Sci. 34, 84–94.
Yu, G.R., Wen, X.F., Sun, X.M., Tanner, B.D., Lee, X.H., Chen, J.Y., 2006. Overview of ChinaFLUX and evaluation of its eddy covariance measurement. Agric. For. Meteorol. 137, 125–137.
Yu, G.R., Zhang, L.M., Sun, X.M., YL, Fu, Wen, X.F., Wang, Q.F., et al., 2008. Environmental controls over carbon exchange of three forest ecosystems in eastern China. Glob. Chang. Biol. 14, 2555–2571.
Yu, G.R., Li, X.R., Wang, Q.F., Li, S.G., 2010. Carbon storage and its spatial pattern of terrestrial ecosystem in China. J. Resour. Ecol. 1, 97–109.
Yu, G.R., Zhu, X.J., YL, Fu, He, H.L., Wang, Q.F., Wen, X.F., et al., 2013. Spatial patterns and climate drivers of carbon fluxes in terrestrial ecosystems of China. Glob. Chang. Biol. 19, 798–810.
Yu, H.X., He, Z.J., Hong, C.Q., 2013. Soil enzyme activity and its relationship with soil nutrient in the Yulong snow mountain. J. Yunnan Agric. Univ. 28, 668–675.
Yu, G.R., Chen, Z., Piao, S.L., Peng, C.H., Ciais, P., Wang, Q.F., et al., 2014a. High carbon dioxide uptake by subtropical forest ecosystems in the East Asian monsoon region. United States of America]–>Proc. Natl. Acad. Sci. U. S. A. 111, 4910–4915.
Yu, G.R., Zhang, L.M., Sun, X.M., 2014b. Progresses and prospects of Chinese terrestrial ecosystem flux observation and research network (ChinaFLUX). Prog. Geogr. 33, 903–917.
Yu, G.R., Ren, W., Chen, Z., Zhang, L.M., Wang, Q.F., Wen, X.F., et al., 2016. Construction and progress of Chinese terrestrial ecosystem carbon, nitrogen and water fluxes coordinated observation. J. Geogr. Sci. 26, 803–826.
Zha, T., Kellomaki, S., Wang, K.Y., Rouvinen, I., 2004. Carbon sequestration and ecosystem respiration for 4 years in a Scots pine forest. Glob. Chang. Biol. 10, 1492–1503.
Zhang, L.M., Yu, G.R., Sun, X.M., Wen, X.F., Ren, C.Y., Song, X., et al., 2006. Seasonal variation of carbon exchange of typical forest ecosystems along the eastern forest transect in China. Sci. China Ser. D: Earth Sci. 49, 47–62.
Zhang, Y.P., Sha, L.Q., Yu, G.R., Song, Q.H., Tang, J.W., Yang, X.D., et al., 2006. Annual variation of carbon flux and impact factors in the tropical seasonal rain forest of Xishuangbanna, SW China. Sci. China Ser. D: Earth Sci. 49, 150–162.
Zhang, Y.P., Tan, Z.H., Song, Q.H., Yu, G.R., Sun, X.M., 2010. Respiration controls the unexpected seasonal pattern of carbon flux in an Asian tropical rain forest. Atmos. Environ. 44, 3886–3893.
Zhang, Z., Zhang, R., Cescatti, A., Wohlfahrt, G., Buchmann, N., Zhu, J., et al., 2017. Effect of climate warming on the annual terrestrial net ecosystem CO_2 exchange globally in the boreal and temperate regions. Sci Rep 7, 3108.
Zhao, L., Li, Y., Xu, S., Zhou, H., Gu, S., Yu, G., et al., 2006. Diurnal, seasonal and annual variation in net ecosystem CO_2 exchange of an alpine shrubland on Qinghai–Tibetan plateau. Glob. Chang. Biol. 12, 1940–1953.
Zhou, G., Liu, S., Li, Z., Zhang, D., Tang, X., Zhou, C., et al., 2006. Old-growth forests can accumulate carbon in soils. Science 314, 1417.
Zhu, Z., Sun, X., Zhou, Y., Xu, J., Yuan, G., Zhang, R., 2005. Correcting method of eddy covariance fluxes over non-flat surfaces and its application in ChinaFLUX. Sci. China Ser. D: Earth Sci. 48, 42–50.
Zhuang, W., Cheng, L., Whitley, R., Shi, H., Beringer, J., Wang, Y., et al., 2016. How energy and water availability constrain vegetation water-use along the North Australian Tropical Transect. Int. J. Plant Prod. 10, 403–423.